https://doi.org/10.5194/egusphere-2023-407
Preprint. Discussion started: 28 March 2023

Impacts of reducing scattering and absorbing aerosols on the temporal extent and intensity of South and East Asian summer monsoon

Chenwei Fang[1, 2, *], Jim M. Haywood[2, 3], Ju Liang[2, 4], Ben T. Johnson[3], Ying Chen[5,6], Bin Zhu[1, *]

[1]Key Laboratory of Meteorological Disaster, Ministry of Education (KLME), Joint International Research Laboratory of Climate and Environment Change (ILCEC), Collaborative Innovation Center on Forecast and Evaluation of Meteorological Disasters, Key Laboratory for Aerosol-Cloud-Precipitation of China Meteorological Administration, Nanjing University of Information Science & Technology, Nanjing 210044, China
[2]Faculty of Environment, Science and Economy, University of Exeter, Exeter, UK
[3]Met Office Hadley Centre, Exeter, UK
[4]College of Resources and Environmental Sciences, China Agricultural University, Beijing, 100193, China
[5]Paul Scherrer Institute, Forschungsstrasse 111, 5232 Villigen, Switzerland
[6]School of Geography Earth and Environment Sciences, University of Birmingham, Birmingham B15 2TT, UK

Correspondence to: Chenwei Fang (fangcw515@163.com) and Bin Zhu (binzhu@nuist.edu.cn)

Abstract. The vast majority of reductions in aerosol emissions are projected to take place in the near future; however, associated impacts on the large-scale circulation over the populated Asian monsoon region remain uncertain. Using the state-of-the-art UK Earth System Model version 1 (UKESM1), this study examines the response of the South Asian and East Asian summer monsoon (SASM and EASM) to idealized reductions in anthropogenic emissions of carbonaceous aerosols and SO_2. The analysis focuses on changes in the monsoon temporal extent and intensity of precipitation following decreases in either scattering (SCT), absorbing (ABS) aerosols, or decreases in both. For SCT, the combination of the early transition of land-sea thermal contrast and sea level pressure gradient during the pre-monsoon season together with the late transition in the post-monsoon season associated with the tropospheric warming, advances the monsoon onset but delays its withdrawal, which leads to an extension of the summer rainy season across South and East Asia. The northward shift of the upper-tropospheric Asian jet forced by the SCT reduction causes the anomalous convergence of tropospheric moisture and low-level ascent over northern India and eastern China. The intensification of the South Asian High (SAH) due to the warming over land also contributes to the dynamic instability over Asia. These changes enhance the rainy season of these regions in boreal summer. Reductions in absorbing aerosol act in the opposite sense, making the Asia's rainy season shorter and weaker due to the opposite impacts on land-sea contrast, Asian jet displacement and SAH intensity. With reductions in both SCT and ABS aerosol together the monsoon systems intensify, as the overall impact is dominated by aerosol scattering effects and results in the strengthening of monsoon precipitation and 850-hPa circulation. Although aerosol scattering and absorption play quite different roles in the radiation budget, their effects on the monsoon precipitation seem to add almost linearly. Specifically, the patterns of monsoon-related large-scale responses from reducing both SCT and ABS together are similar to the linear summation of separate effect of reducing SCT or ABS alone, despite of the inherent nonlinearity of the atmospheric systems. Our findings suggest that

https://doi.org/10.5194/egusphere-2023-407
Preprint. Discussion started: 28 March 2023

emission controls that target e.g. emissions of black carbon that warm the climate would have a different response to those that target overall aerosol emissions.

1 Introduction

In addition to anthropogenic greenhouse gas (GHG), it has long been established that aerosol emissions are important external climate forcing that strongly modulates regional climate (e.g. Taylor and Penner, 1994). Previous research has investigated the responses of regional precipitation to the changes in the emissions of aerosols and GHGs, where higher sensitivities are usually seen for the aerosol-forced responses (Kloster et al., 2009; Liepert et al., 2004; Persad et al., 2022), particularly in regions with high aerosol emissions (Samset et al., 2018). Anthropogenic aerosols can also alter the atmospheric circulation at hemispheric and regional scales due to its inhomogeneous distribution (Cox et al., 1995; Diao et al., 2021). One of the regions where the general circulation is strongly affected by the perturbation of aerosol concentrations is the Asian monsoon region (Jiang et al., 2013; Lau et al., 2017; Li et al., 2018; Salzmann et al., 2014; Undorf et al., 2018). It contributes nearly 20% of global anthropogenic aerosols emissions (Grandey et al., 2018), covers over 20% of the Earth's land and contains almost 60% of the world's population exposed to monsoon-related climate extremes (Li et al., 2016). Hence, deepening the understanding of the aerosol-related regional climate changes over this region is important for supporting the local communities in coping with possible risks of climate extremes under future changes in external climate forcing.

The South and East Asian summer monsoons (SASM and EASM) are two of the most influential monsoon systems in the world (Ha et al., 2017). The SASM originates from the northward shift of intertropical convergence zone (ITCZ) and is mainly observed in the tropics, while the EASM has both tropical and subtropical monsoon characteristics (Huang et al., 2017). Previous studies have shown that changes in the anthropogenic aerosol emissions from both local and remote sources can lead to the observed predominant decreased SASM circulation and precipitation during the late twentieth century (Bollasina et al., 2011; 2014). Ganguly et al. (2012) further demonstrated that the fast response of SASM to changes in aerosol emissions dominates the drying trend in precipitation over the highly populated central-northern Indian region compared with the slow feedbacks associated with aerosol-induced changes in sea surface temperature (SST). However, changes in summer precipitation vary on a regional basis over East Asia with the weakened low-level wind, featuring a decrease in central and northeast China but an increase in the south China and Yangtze River valley in the late 20th century (Li et al., 2016). Anthropogenic aerosols also play a crucial role in the spatial pattern of EASM adjustments (Menon et al., 2002; Rosenfeld et al., 2007; Jiang et al., 2013; Song et al., 2014; Wang et al., 2017). Interestingly, the weakened wind and accompanying EASM precipitation changes are also modulated by the atmospheric response to aerosol forcings, though the SST cooling also contributes (Wang et al., 2017; Wang et al., 2019). Considering the prominent contributions of the fast atmospheric adjustments to the aerosol-induced changes in both SASM and EASM, this study mainly examines the fast monsoon responses to aerosol emission perturbations.

https://doi.org/10.5194/egusphere-2023-407
Preprint. Discussion started: 28 March 2023

Globally, emissions of anthropogenic aerosols and their precursors have been declining for the last few decades and the increasing trend of aerosol emissions in many regions of Asia have reversed or are projected to reverse due to technological advances, socioeconomic progress and policy control (Wang et al., 2012; Westervelt et al., 2018). For instance, global emissions of black carbon (BC, absorbing aerosol) and sulfur dioxide (SO_2, precursor of scattering aerosol sulfate) in 2100 are projected to decline by 70-90% from 2015 under the medium and strong pollution controls of the Shared Socioeconomic Pathways (SSPs; Lund et al., 2019). In the Asian monsoon region, SO_2 and BC emissions have declined by 75% and 30% respectively over China in the last decade (Li et al., 2017; Zheng et al., 2018). Sulfate and BC burdens over South Asia in 2100 are also assumed to decrease by 11-69% and 0.6-88% respectively compared to those at present day under high- to low-emission scenarios (SSP3-7.0, SSP2-4.5 and SSP1-1.9; Lund et al., 2019). Many studies based on multi-models have considered the global and regional climate adjustment under different levels of air pollution control (e.g., Kloster et al. 2009; Wang, Z. et al., 2016; Xing et al., 2016; Westervelt et al. 2018; Wilcox et al., 2020). However, the potential changes of EASM and SASM caused by anthropogenic aerosol reductions and the corresponding causal mechanisms have received less attention. In particular, although the physical impacts of scattering (SCT; e.g., sulfate) or absorbing (ABS; e.g., BC) aerosol types are very different (e.g. Li, J. et al., 2022), the impacts of reducing sulfate precursor emissions relative to BC in possible Asian monsoon adjustments remains unclear. Using Community Earth System Model, Zhao et al. (2018) showed a warmer and wetter Asian monsoon region with increased extreme precipitation events under Representative Concentration Pathway 8.5 scenario but did not focus on the EASM and SASM responses to the change of individual aerosol species.

Besides, most studies focusing on the modulations of EASM and SASM by anthropogenic aerosols only involved the seasonal climate adjustments in summer or winter. Bollasina et al. (2013) pointed out that the anthropogenic aerosols can also lead to sub-seasonal changes to the activity of monsoon systems, i.e., the onset of SASM in spring is observed to become earlier during the late 20th century and this change is attributed to the increases in the emissions of anthropogenic aerosols. Wang, D. et al. (2016) also reported that the direct effects of BC or the combination of BC and sulfate can bring forward EASM onset due to the deep heating in the middle-upper troposphere in spring. However, it remains unclear how the reductions of SCT and ABS aerosols affect the onset and withdrawal dates of the EASM and SASM. Whether the temporal extent of EASM and SASM will be prolonged or shortened due to the aerosol emission reductions is still unclear.

Considering the difference in the mixing states of aerosol types due to the varying regions and environments, the monsoon responses to the total anthropogenic aerosol forcings may not be a simple linear superposition of the forcings from ABS and SCT aerosols (Ji et al., 2011). Herbert et al. (2021) found that the response of Asian summer monsoon to simultaneous aerosol emission reductions in both South and East Asia differs from the sum of responses to the aerosol reduction in each subregion according to the simulation from an Intermediate Global Circulation Model, implying the nonlinear response of Asian summer monsoon to regional reductions of aerosol emissions. However, the responses of the Asian summer monsoon to the reduction of total anthropogenic aerosols and different aerosol types and their potential linear combination remain unexamined. Also, further investigations are still required to understand which aerosol types plays the dominant role in shaping the response of EASM and SASM to anthropogenic aerosol reductions.

https://doi.org/10.5194/egusphere-2023-407
Preprint. Discussion started: 28 March 2023

Impact by the COVID pandemic, a significant global reduction in aerosol and GHGs emissions has been observed in recent years (Lal et al., 2020; Liu et al., 2020), which appears to affect global and regional climates (Le et al., 2020; Li et al., 2020; Yang et al., 2020), inspiring us to assess the potential climate adjustments to a temporary short-term perturbation of anthropogenic aerosol emissions. In a recent study by Fahrenbach and Bollasina (2022), the strong contribution from abrupt and rapid near-term aerosol emission changes to large-scale climate adjustments at short timescales (i.e. monthly) via rapid circulation adjustments was highlighted. The signal of this aerosol-induced hemispheric-wide climate adjustments on short timescales are even consistent with longer-term (decadal) trends according to their study. Hence, this study examines and compares the responses of the EASM and SASM patterns to the short-term emission reductions of total anthropogenic aerosols as well as the SCT and ABS types using the state-of-the-art UK Earth System Model version 1 (UKESM1). The temporal and spatial responses of the large-scale monsoon systems and the environmental mechanism behind these responses are investigated. Furthermore, the linear relationships between the impacts of emission reductions in different aerosol types will be discussed. The experiment design and the configurations of the UKESM1 model are described in Section 2. Section 3 presents results of model verification and experiments quantifying the respective impacts of reducing total aerosols and different aerosol types on the temporal extent and intensity of SASM and EASM. Section 4 summarize and discuss the findings of this study.

2 Methods

2.1 Model

This study uses the UKESM1 as described by Sellar et al. (2019). The modelling system includes the physical core climate model of HadGEM3-GC3.1 (Hadley Centre Global Environment Model version 3; Kuhlbrodt et al., 2018; Williams et al., 2018) and the UKCA model (U.K. Chemistry and Aerosols model; Archibald et al., 2020; Mulcahy et al., 2018), along with terrestrial carbon and nitrogen cycles, dynamic vegetation and interactive ocean biogeochemistry. As a successor to HadGEM2-ES (Hadley Centre Earth System Model; Collins et al., 2011), UKESM1 introduces an improved representation of aerosol radiative forcing with a prognostic aerosol scheme interacting with radiation and cloud microphysics and a prognostic atmospheric chemistry scheme, allowing improved representation of the climate responses to short-lived climate forcers (e.g., methane, tropospheric ozone and BC) reductions (Stohl et al., 2015). The model's resolution is 1.25° in latitude and 1.875° in longitude and with 85 hybrid height layers from surface to 85 km.

The interactive aerosols are simulated with GLOMAP-Mode (Global Model of Aerosol Processes; Mann et al., 2010), a double-moment modal aerosol microphysics scheme that represents sulphate, BC, organic carbon (OC) and sea salt across five log-normal size modes, while mineral dust is simulated with the bin emission scheme of Woodward (2001). Atmospheric chemistry is simulated using the unified stratospheric-tropospheric (StratTrop) chemistry, which combines the stratospheric scheme (Morgenstern et al., 2009; 2017) and the tropospheric chemistry (O'Connor et al., 2014). Aerosol radiative effects in both the shortwave and longwave spectral regions are included (Bellouin et al., 2013). Aerosol-cloud interactions are simulated

https://doi.org/10.5194/egusphere-2023-407
Preprint. Discussion started: 28 March 2023

using the UKCA-Activate scheme (West et al., 2014). For the simulations used here, the prescribed GHG concentrations (including CFC-12, CH_4, CO_2, HFC-134 and N_2O, etc.) are from the Coupled Model Project Intercomparison Phase 6 (CMIP6; Meinshausen et al., 2020) under the SSP3-7.0 scenario; for more details see O'Connor et al. (2021).

2.2 Experimental Design

Four sets of simulations were conducted in this study. Each comprised a 10-member ensemble of UKESM1 simulations that ran for 5 years from 2020 to 2024. In the control set all forcings and aerosol emissions were based on the CMIP6 SSP3-7.0 scenario (Rao et al., 2017), which arguably represents one of the possible "worst"' future pathways for air quality with weak pollution controls and low levels of technology development. Lund et al. (2019) estimated that the total aerosol forcing in 2100 relative to 1750 is -0.51 W m^{-2} in SSP3-7.0, which is similar to estimates of the preindustrial to present-day level (IPCC, 2021). Hence, the control simulations based on SSP3-7.0 scenario represent a high baseline from which to assess the maximum climate response to strong pollution mitigation.

To investigate the theoretical impacts that short-term pollution mitigation may have, three other sets of simulations were performed in which aerosol emissions were perturbed in different ways. In the "Total" set, all anthropogenic emissions of SO_2, organic matter (OM) and BC were reduced by 75% relative to the SSP3-7.0 scenario. This included perturbing emissions from all fossil fuel and biofuel sources but not from biomass burning. In the "SCT" set only the SO_2 and OM emissions were reduced (again by 75% relative to SSP3-7.0) to decrease the loading of sulphate and organic aerosols that pre-dominantly scatter solar radiation. In the "ABS" set only the BC was reduced (by 75% relative to SSP3-7.0), which substantially decreases the absorption of solar radiation by aerosol. BC was the only anthropogenic aerosol component in the model to absorb significantly in the solar spectrum. The aim of selectively reducing aerosol scattering and absorption was to understand the role of these different aerosol-radiative interactions on the monsoons, whereas the Total experiment allowed us to investigate if reducing scattering and absorbing together gives a different response compared to summing effects from reducing them separately.

In each of the perturbed sets the aerosol reductions were applied globally but only for the first 2 years of the simulations, after which emissions returned to the levels set by the SSP3-7.0 scenario. Only the first 2 years of the perturbed simulations were used in this study, whereas the data from the final 3 years offer opportunities for follow-on studies to look at the response to suddenly withdrawing pollution controls. To create the 10 member ensembles within each set the individual simulations ran with different random perturbations in the stochastic physics, causing the atmospheric flow to diverge into different meteorological realizations. Using the first 2 years of each simulation gives us the equivalent of a 20 years sample from each set, allowing a statistically more significant picture of the climate in the control case and those with the aerosol emissions perturbations.

It should be noted that the model includes aerosol-radiation interactions, aerosol-cloud interactions and surface albedo effects, but this study will mainly discuss aerosol-radiation interactions. To evaluate the performance of UKESM1 in simulating the Asian summer monsoon we also use precipitation and wind fields from the period 1985-2014, obtained from the UKESM1 historical simulations in the CMIP6 database (https://esgf-node.llnl.gov/search/cmip6/). The basic model configuration and

https://doi.org/10.5194/egusphere-2023-407
Preprint. Discussion started: 28 March 2023

resolution of the UKESM1 historical simulations are consistent with the simulation settings used in this study except for aerosol emissions and time-varying forcings. To evaluate precipitation over the SASM and EASM regions we also use observational precipitation data from both the Climate Prediction Center (CPC) unified gauge-based daily observations (Chen et al. 2008) and the Global Precipitation Climatology Project (GPCP) rain gauge-satellite combined precipitation dataset (Huffman and Bolvin, 2013). Precipitation and wind fields from the ECMWF's (European Center for Medium-Range Weather Forecast) Fifth-generation Reanalysis (ERA5; Hersbach et al., 2020) are also used in comparisons against the model simulations.

3 Results

3.1 Model evaluation

The performance of UKESM1 in representing the tropospheric environment has been verified with respect to climate observations, including the variations in aerosol optical depth and atmospheric fields (including temperature, sea level pressure, precipitation and wind fields) on global and regional scales (Mulcahy et al., 2018; Archibald et al., 2020; O'Connor et al., 2021). As our focus is primarily on the monsoon, here the model performance is evaluated by comparing against observations of the regional precipitation over South and East Asia. As our study involves the sub-seasonal variations in monsoon onset and withdrawal, the monthly comparisons among South and East Asia precipitations from CPC and GPCP observations, ERA5 reanalysis and the UKESM1 simulations are shown in Fig. 1. The mean values of observations from the GPCP and CPC datasets are shown as black dots. Simulated precipitation over South Asia from the UKESM1 model shows higher correlations (0.69-0.81) from July to September with observations than that (0.54-0.58) from May to June, indicating the better performance of UKESM1 in reproducing the summer and early autumn precipitation, although all correlations are statistically significant ($p < 0.001$). The precipitation variations over East Asia are also effectively reproduced by the model with correlations of 0.63-0.86 ($p < 0.001$). The standard deviation (STD) reflects the variation range of the dataset. A normalized STD ($STD_{model}/STD_{observations}$) value of 1 indicates the same varied amplitude between the simulations and the observations. The normalized STD values range from 0.98-1.49 over South Asia and 1.06-1.38 over East Asia from May to September, which is within the range of 0.4-2.0 calculated from the simulated climatological mean summer precipitation based on CMIP5 and CMIP6 climate models in Xin et al. (2020) who performed comparisons over East Asia. The root-mean-square deviation (RMSD) indicates the departure between the simulations and observations. Khadka et al. (2021) showed that the RMSE ranges based on CMIP5 and CMIP6 models are 2.18-4.01 and 1.91-6.0 mm day^{-1}, respectively, over Southeast Asian monsoon region. The RMSE range between the UKESM1 simulation and observation is 3.04-5.35 and 1.37-2.26 mm day^{-1} over South and East Asia, respectively, which is within the RMSE range of CMIP6 models.

Fig. 2 shows the wind fields over Asia continent during pre-monsoon (April-May), monsoon (June-August) and post-monsoon seasons (September-October). The selection of the different monsoonal periods follows previous studies (Vissa et al., 2013; Zeng et al., 2019; Zhou et al., 2020). Overall, the model captures the spatial features and temporal evolutions of the ASM

https://doi.org/10.5194/egusphere-2023-407
Preprint. Discussion started: 28 March 2023

horizontal circulations from upper to lower levels. However, it should be noted that the simulated upper-level westerly jet northward of 40°N from pre- to post-monsoon seasons are stronger compared to ERA-5 reanalysis (Fig. 2g-i). The lower-level southwest monsoon flow over South Asia is also overestimated in the model, while the monsoon southerly wind prevailing over East Asia is slightly underestimated (Fig. 2q).

3.2 Response of monsoon temporal extent and intensity

Monsoon transition is usually referred to as the seasonal shift of wind direction between the dry and wet seasons (Zhao et al., 2006). The change of some key climatic variables in the monsoon region is often used to define the onset and withdrawal pentad (5-day mean) or day of the SASM and EASM (e.g., He and Zhu, 2015; Noska and Misra, 2016; Wang, D. et al., 2016). Note that the SASM and the continental part of the EASM are regarded as tropical and subtropical monsoons, respectively, and their seasonal wind reversals are mainly characterized by the changes of zonal and meridional winds (Sun and Ding, 2011). Fig. 3 shows the variations in monsoon duration and monsoon precipitation of SASM and EASM induced by the modelled aerosol reductions. The monsoon duration and the precipitation for the duration can be obtained by calculating the monsoon onset and withdrawal dates. The monsoon onset/withdrawal dates were derived according to the definitions given in previous studies, as detailed below. The monsoon changes showing in Fig. 3 were calculated based on different definitions to demonstrate that the variations of the monsoon temporal extent and intensity are clearly shown in different definitions. Here we adopted the definitions from Wang et al. (2009) and Noska and Misra (2016), hereafter referred to as W2009 and N2016, to obtain the SASM onset and withdrawal dates in Fig. 3(a) and (b), respectively. W2009 used 850-hPa zonal wind averaged over South Asia (5-15°N, 40-80°E) as an onset circulation index (OCI) of the SASM, and the date of onset is defined as the first day when OCI exceeds 6.2 m s^{-1}. N2016 in Fig. 3(b) used All-India rainfall (AIR) to calculate the cumulative daily anomaly $C'_m(i)$of AIR for day i of year m: $C'_m(i) = \sum_{n=1}^{i}[AIR_m\ (n) - \bar{\bar{C}}]$, where $\bar{\bar{C}}$ is the climatology of the annual mean of AIR over N (=360 based on UKESM1's calendar) days for M (=2) years. The onset/withdrawal of SASM is defined as the day after $C'_m(i)$ reaches its absolute minimum/maximum.

The SASM duration and precipitation in Fig. 3(a) and (b) show similar changes, although they are based on different definitions. Compared to the SASM in the control case, reduction in SCT extends the temporal extent of the SASM duration and enhances the monsoon precipitation, while reduction in ABS shortens the SASM and reduces the monsoon precipitation. With the combined effects induced by SCT and ABS aerosols, reduction in total aerosols has negligible impacts on the temporal extent of SASM and enhances the monsoon precipitation although the enhancement is weaker than pure SCT reduction.

Definitions from Wang, D. et al (2016) and Guo (1983), hereafter referred to as W2016 and G1983, are applied in Fig. 3 (c-d) to calculate the EASM monsoon duration and precipitation. The 850-hPa meridional wind (V_{850}) over East Asia was used in W2016 to determine the EASM onset and withdrawal: (1) the onset pentad of the EASM is the pentad when V_{850} over East Asia starts to be greater than 0 m s^{-1} (i.e. a net southerly component) and remains positive in the subsequent three pentads (or the average V_{850} of the accumulative four pentads is greater than 0.5 m s^{-1}) ; (2) the withdrawal pentad of the EASM is the

https://doi.org/10.5194/egusphere-2023-407
Preprint. Discussion started: 28 March 2023

pentad when V_{850} turns negative (i.e. a net northerly component). The EASM onset/retreat pentad based on G1983 was calculated as the difference between the sea level pressures over land (representing by 110°E) and sea (representing by 160°E) over East Asia. The impacts of reducing SCT and ABS on the EASM in terms of timescale and intensity (here is characterized by precipitation amount) are similar to that on the SASM, except that the reduction in total aerosol slightly shortens the temporal extent of the EASM (more pronounced in G1983) and increases the summer precipitation over the EASM-controlled region.

Fig. 4 and 5 show the spatial patterns of the opposing changes in the precipitation and the 850-hPa circulation of the SASM and EASM induced by the SCT and ABS reductions. The monsoon changes are consistent over most of South Asia, showing the increased (decreased) precipitation and the stronger (weaker) monsoon circulation due to SCT (ABS) reduction. The anomalies of monsoon precipitation and circulation over for EASM are more complicated. Accompanied by the abundant moisture brought by the stronger southwesterlies from Bay of Bengal and Indian Ocean, reduction in SCT increases the precipitation over most parts of eastern China, especially over the southern part. Reduction in ABS mainly induces a decrease of precipitation in different subregions over East Asia. There are also some regions with increased anomalous precipitation, but it was not statistically significant in this study ($p < 0.05$). In general, the impacts of the SCT reductions dominate both the SASM and EASM adjustments related to the monsoon precipitation and circulation changes induced by short-term total aerosols mitigation.

To determine the SASM and EASM duration changes, the variations in monsoon onset and withdrawal dates are further examined (Fig. 6). The mean values and the 25th-75th percentile ranges of the monsoon onset date, withdrawal date and duration over South and East Asia are also summarized in Table S1. Reduction in SCT advances the SASM onset but delays the SASM withdrawal, thus extending the SASM duration to a certain extent (0.4 pentads in W2009 and 11.4 days in N2016); yet reduction in ABS tend to delay the SASM onset (more pronounced in W2009) and advance the SASM withdrawal, thus shortening the SASM duration by 2 pentads (W2009) or 3.2 days (N2016). Regarding the EASM changes, the monsoon duration is extended by 0.9 pentads in W2016 and 1 pentad in G1983 due to the reduction in SCT, which is mainly contributed by the monsoon withdrawal deferment. Reduction in ABS oppositely advances the withdrawal, leading to a shorter monsoon (0.9 pentads in G1983) in East Asia. Compared to the distinguishable EASM withdrawal adjustments, the SCT- or ABS-reduction induced EASM onset adjustments calculated by W2016 (based on meridional wind) and G1983 (based on land-sea pressure difference) are not obvious and consistent, indicating the complexity of EASM onset. He et al. (2008) also pointed out that the EASM exhibits a progressive and complicated establishment and a swift withdrawal. Simultaneously influenced by the SCT and ABS reductions, reduction in total aerosol shows limited impacts on the SASM onset and withdrawal (advances the SASM onset in N2016). Compared to the changes in SASM seasonal transition, the EASM onset date is postponed but the withdrawal date is advanced due to the aerosol reduction, hence the EASM temporal extent is shortened a little (0.5 pentad in W2016 and 1.4 pentad in G1983).

https://doi.org/10.5194/egusphere-2023-407
Preprint. Discussion started: 28 March 2023

3.3 Responses of the monsoon-related large-scale environments

3.3.1 Responses of land-sea contrast

We now examine how the atmospheric adjustments regulate the duration and intensity of the SASM and EASM due to the aerosol reductions. Figure 7 shows the time-altitude cross sections of air temperature anomalies for emission reductions in different aerosol types averaged over South and East Asia. The division of South and East Asia (Fig. S1) used in this study follows Iturbide et al. (2020), which is defined for the sixth IPCC assessment report. The weakened aerosol scattering significantly increases the tropospheric temperature over South and East Asia land throughout the year, while the ABS reduction leads to a decrease in air temperature in the tropospheric due to the weakened absorption of shortwave radiation. This air temperature increase (decrease) due to the SCT (ABS) reduction over Asia during pre- and post-monsoon seasons is favourable for early (late) transition of land-sea thermal contrast in spring and late (early) transition in autumn, provoking the early (late) monsoon onset and late (early) withdrawal (Wang, D. et al., 2016). The adjusted land-sea thermal contrast contributes to the significant sea level pressure (SLP) anomalies over the Asian continent and the adjacent oceans during pre-monsoon, monsoon and post-monsoon seasons (Fig. 8). The SCT reduction induced land warming yields a lower SLP anomaly over Asia continent compared with that over Indian and western Pacific oceans, which is favourable for the early/late transition of land-sea pressure difference in pre/post-monsoon season and a stronger SASM and EASM circulation in monsoon season. In contrast, the ABS reduction leads to a higher magnitude of SLP anomalies over Asian land from pre- to post-monsoon seasons; hence, the land-sea SLP gradient reversal is delayed in pre-monsoon season but advanced in post-monsoon season, thus shortening the duration of both the SASM and EASM. The reduced land-sea pressure contrast during monsoon season also weakens the Asian monsoon intensities.

In addition, the anomalous land-sea SLP gradient between the Asian continent and the Indian and the western Pacific Oceans caused by the short-term total aerosols mitigation during monsoon season is dominated by the SCT aerosols and enhances the monsoon circulation over South and East Asia (Fig. 8e). In other seasons except summer, the land-sea SLP adjustments over Asia is controlled by the combined effects of SCT- and ABS-reductions (Fig. 8a and 8i). The stronger impact of the ABS-reduction may be due to the higher emission of ABS aerosols (e.g., BC) in the winter half year compared with that in summer, which allows a bigger effect from ABS-reduction.

3.3.2 Responses of the upper-tropospheric systems

For the upper troposphere, we first analyze the responses of the subtropical westerly jet (SWJ) and tropical easterly jet (TEJ) to the reduction in different types of aerosols as these systems are recognized as one of the major circulation systems controlling the Asia climate. Numerous studies have suggested that the summer drought and flood in Asia are closely related to the location and intensity of the upper-tropospheric jet (e.g., Chiang et al., 2017; Madhu, 2014; Xie et al., 2015). However, CMIP6 analysis from Dong et al. (2022) showed that the anthropogenic aerosols were likely the primary driver of summer jet adjustments. The responses of the South Asian High (SAH) governing the Tibetan Plateau during boreal summer is also considered. The strong

https://doi.org/10.5194/egusphere-2023-407
Preprint. Discussion started: 28 March 2023

association between the variations in the SAH and Asia precipitation anomalies have been proved based on reanalysis and observations (Cai et al., 2017; Wang, L. et al., 2016; Wei et al., 2015; 2017; 2021).

Fig. 9 shows the responses of zonal-mean geopotential height over South (70-90°E) and East Asia (100-120°E) during monsoon season according to the definitions of W2009 and W2016. Coherent with the temperature perturbations shown in Fig. 7, both the geopotential height changes over South and East Asia during monsoon season caused by the emission reduction of total aerosols are dominated by the atmospheric cooling associated with the SCT reduction. The pressure increases in the uppermost troposphere (200-500 hPa) north of 40°N over South and East Asia, which strengthens (weakens) the poleward pressure gradient force in the north (south) flank of this area. The SWJ axis is centered around 40°N in summer with central values of 25-30 m s^{-1} at 200-hPa level (Yu et al., 2021), as shown in Fig, 10 and Fig. 11 (a). Therefore, the strengthened pressure gradient force north of the SWJ center induced by the total aerosol/SCT reduction accelerates the westerlies in the north flank of the jet center (north of 40°N over South Asia and north of 50°N over East Asia), and thus the SWJ moves northward over Asia. As can be seen in Fig. 11(a), the strength of TEJ (centered between 10°N and 20°N) is much weaker than that of SWJ. The weakened poleward pressure gradient south of 40°N leads to a negative zonal wind anomalies over South and East Asia when reducing total or SCT aerosols, leading to the northward shift of the TEJ over South Asia. On the contrast, reduction in ABS decreases the pressure in the uppermost troposphere north of 40°N and weakens (strengthens) the poleward pressure gradient force in the north (south) flank of the SWJ center, inducing the accelerations of the westerlies in the south flank of the jet center and the southward displacement of the Asian jet over South and East Asia. The geopotential height and upper-tropospheric jet changes in monsoon season based on other definitions (N2016 and G1983) are shown in Fig. S2 and S3, which have consistent meridional variations with those presented in Fig. 9 and 10.

The meridional shift of the Asian jet and the variations in 200-hPa horizontal circulation field caused by the emission reductions in different aerosol types in monsoon season can be seen more clearly in Fig. 11. The SCT reduction leads to a long and narrow westerly (easterly) anomaly over the Asian continent north (south) of 40°N at 200-hPa, encompassing the South and East Asia, whilst the ABS reduction yields the opposite changes. The change of Asian jet at 200-hPa caused by SCT reduction induces a broad high-level divergence over South and East Asia, which motivates the moisture convergence in the whole layer and low-level upward motion (Fig. 12e and 12f). Therefore, an increased monsoon precipitation is found over South (Fig. 4c and 4g) and East Asia (Fig. 5c and 5g). In addition, located in the central part of the South Asia, monsoon trough is the portion of the intertropical convergence zone that extends into a monsoon circulation. The monsoon-trough-controlled area is usually the region with heavy precipitation due to its resulting cyclonic vorticity at lower level (Mishra et al., 2012). According to the configuration of the enhanced divergence at the upper level (Fig. 11d) and increased vertical velocity (Fig. 12e), the monsoon trough is enhanced, thus creating strong dynamic conditions for precipitation over northern South Asia.

The ABS reduction-induced easterly anomalies to the north and westerly anomalies to the south of 40°N in contrast generates the high-level convergence anomalies over northern South Asia and East Asia (Fig. 11e). The resulting moisture divergence in the whole layer and low-level downward motions over northern South Asia and most of East Asia hinder the regional monsoon precipitation (Figs. 11g and 11h). Following the impacts of the SCT reduction, emission reduction in total aerosols

https://doi.org/10.5194/egusphere-2023-407
Preprint. Discussion started: 28 March 2023

also contributes to the northward shift of the Asian jet, but the westerly anomaly north of 40°N and the accompanying upper-tropospheric divergence are weaker than that of reducing the SCT alone.

Fig. 13 compares the SAH changes induced by the short-term emission reductions in different aerosol types. The SAH gets stronger and moves northward when only the SCT is reduced, which could be attributed to the land warming over Asia. The land cooling induced by the ABS reduction leads to a weaker SAH, but the SAH change is incomparable to that with the SCT-reduction. Owing to the dominant effects of the SCT reduction, reduction in total aerosols enhances the SAH intensity over Asia. Using reanalysis and observation data, Wei et al. (2015; 2017; 2021) conducted a series of studies and revealed that the northwestward (southeastward) shift of the SAH is closely related to more (less) Indian summer monsoon precipitation, more (less) north and south China precipitation and less (more) Yangtze River valley precipitation. The SAH intensity is also positively related with monsoon precipitation over India, as reported in their studies. Along with the reduction of total or SCT aerosols and the resulting enhanced and northward moving SAH, the spatial pattern of summer precipitation anomalies over South and East Asia (Fig. 4 and 5) are consistent with their results. The easterly anomalies to the south of the enhanced SAH center (with the climatological value of more than 16800 gpm at 100-hPa) cause a stronger vertical wind shear over the northern South Asia and southern East Asia due to the total or SCT reductions. The change in vertical wind shear has important impacts on the convective development by altering the dynamic instability (Wang et al., 2019). As a result, the intensity of the local convective systems is increased due to the strengthened dynamic instability over South and East Asia.

3.4 Linear combination of the impacts from the emission reductions in different aerosol types

Future global emission reductions of the SCT and ABS aerosols may not be synchronous due to the differences in contributing region and sector sources, technological progress and air pollution policies (Li, H. et al., 2022; Rao et al., 2017). However, The SASM and EASM responses to the reductions in total aerosols may not a linear summation of the impacts of the reductions in individual aerosol type due to the nonlinearity of the atmospheric systems. Therefore, we compare the results summed from the sensitivity experiments of reducing SCT or ABS alone with those of reducing both of them simultaneously to estimate the importance of the nonlinear atmospheric adjustments on the monsoon changes in the future and investigate the respective theoretical impacts of simultaneous or non-simultaneous emission reductions of the SCT and ABS aerosols on the Asian region. Generally, the pattern of the anomalous precipitation and monsoon horizontal circulation over South and East Asia by adding the results of reducing SCT and ABS aerosols are similar to the results of reducing total aerosols (Fig. 4 and 5). But the precipitation in some regions show a reduction in the linear addition compared to the precipitation change in the simulation of reducing total aerosols, although most of the reduced precipitation did not pass the significance test ($p < 0.05$). Besides, the difference in monsoon precipitation and circulation anomalies between linear addition and simulation of simultaneous emission reduction is greater based on the definition from N2016 (Fig. 4f) compared with that using other definitions (Fig. 4b, Fig.5b and 5f). Different from the pentad mean values adopted in other definitions, N2016 uses the daily mean values, which could give rise to the overlay of nonlinearity effects and a larger deviation. For the adjustments of air temperature (Fig. 7), land-sea SLP difference (Fig. 8), geopotential height (Fig. 9), upper-tropospheric jet (Fig. 11), moisture divergence field (Fig. 12) and

https://doi.org/10.5194/egusphere-2023-407
Preprint. Discussion started: 28 March 2023

SAH (Fig. 13) over Asia, the distribution and general feature of the linear addition are also coherent with the results of reducing the total aerosols, yet the variation range of most of the monsoon-related large-scale environments adjustments caused by aerosol emission reductions reflected by the linear addition is greater than that in reducing total aerosols. Various complex nonlinear interactions in the atmosphere (the mixing states of the SCT and ABS aerosols, the nonlinear changes in cloud fields induced by activated aerosols and other feedback from atmospheric thermal and dynamic processes) could contribute to the deviation. Kloster et al. (2008) showed that the aerosol number concentrations of the accumulated particles is more efficiently reduced in the sum of the two experiments that with individual emission reduction of the SCT or ABS compared to the experiment with simultaneous emission reductions. Therefore, the climate adjustments range in the monsoon region is greater in the linear addition results because of the more effective reduction in aerosol number. The difference of the monsoon precipitation and circulation anomalies related to the atmospheric adjustments between the results from linear addition and the simulation with total aerosol reduction is more pronounced over South Asia compared to that over East Asia, indicating that the climate adjustments over South Asia show higher non-linearity. However, the non-linearity hardly affects the general pattern of the Asian monsoon and monsoon-related large-scale environmental adjustments caused by short-term aerosol emission reductions.

4 Conclusions and discussions

The urgent need to mitigate global climate and environmental issues is likely to force drastic GHGs and aerosols emission reductions at the global scale through policy controls and technological innovations in the coming decades. The aerosol-forced temperature and precipitation anomalies dominate the global response when both emissions of carbon dioxide and aerosol were reduced (Fyfe et al., 2021). Hence, the potential signals and the effect mechanisms of short-term air pollution mitigation on the SASM and EASM in terms of the temporal extent and intensity are investigated based on UKESM1 simulations forced by reducing global aerosol emissions by a substantial fraction. The respective responses of different properties of the SASM and EASM to emission reductions in SCT and ABS aerosols are presented. The monsoon sensitivities to simultaneous and non-simultaneous emission reductions of the SCT and ABS aerosols are discussed.

There exists a large degree of similarity in the SASM and EASM responses to the aerosol emission reductions either in temporal or spatial scale. The SCT reduction-induced tropospheric warming and ABS reduction-induced tropospheric cooling over SASM- and EASM-controlled regions happens throughout the year. The warming (cooling) induced by the SCT (ABS) reduction over South and East Asia during pre- and post-monsoon seasons favors early (late) transition of land-sea thermal contrast and SLP gradient in spring and late (early) transition in autumn, thus extending (shortening) the monsoon by advancing (delaying) its onset and delaying (advancing) the withdrawal. The change in pressure gradient force induced by SCT (ABS) aerosol reduction leads to an increase (decrease) in westerlies to the north of the upper-tropospheric jet center, leading to the northward (southward) displacement of the high-level easterly and westerly jet. The northward (southward) displacement of the high-level jet causes the anomalous moisture convergence (divergence) and upward (downward) motion at the lower level

https://doi.org/10.5194/egusphere-2023-407
Preprint. Discussion started: 28 March 2023

over north India and east China, eventually enhancing (weakening) the precipitation over South and East Asia during monsoon season. The stronger (weaker) SAH due to the land warming (cooling) induced by the reduction of SCT (ABS) also facilitates (hinders) the local convective development over northern South Asia and southern East Asia.

Overall, reduction in SCT makes the rainy season over South and East Asia longer and stronger, while reduction in ABS makes the rainy season shorter and weaker. The aerosol-reduction-induced monsoon intensity changes over South and East Asia are dominated by the impacts of reducing SCT, while the onset and withdrawal dates adjustments of the SASM and EASM are controlled by the combined impacts of reducing SCT and ABS aerosols. The difference in magnitude between the linear summation of reducing a certain type of aerosols alone and the results of reducing total aerosols indicates the non-linearity of the whole system (e.g., the non-linear interactions among aerosols). However, the spatial features of the linear summation of the individual effect from reducing SCT or ABS alone is similar to the effect of reducing both aerosol types simultaneously. Considering the unpredictable technological progress and policies, the emission reduction pathways of scattering and absorbing aerosol components are possibly non-synchronous. The opposite adjustments of Asian rainy season forced by scattering and absorbing aerosol emission control and the performance of their linear summation need to be considered during the climate and environment policy-making process.

In this study, we have attempted to investigate the signal of possible responses of different monsoon systems to a hypothesized air pollution mitigation by reducing aerosol emissions globally by a substantial fraction (75%). Although the emission perturbations we apply here are hypothetical and are likely to be larger than those that will actually be implemented, our results illustrate the maximum extent of monsoon adjustments that emission reduction of different aerosol types might be expected to induce. Previous research has estimated that the annual global emissions of BC, SO_2 and organic carbon in 2100 are projected to decline by 64-91%, 56-74% and 8-30%, respectively, compared to 2015 in SSP1-1.9, SSP2-4.5 and SSP3-7.0 scenarios (Lund et al., 2019). Hence, the variation range of plausible responses of the SASM and EASM in terms of duration and intensity may be similar or smaller than the simulated responses presented here. Besides, the resulting monsoon response depends on the model performance in reproducing the location, intensity and evolution of monsoonal characteristics. We have verified that the precipitation intensity and the locations of the associated upper and lower level circulation systems can be reasonably reproduced before, during and after the Asian monsoon season in UKESM1. However, the low-level monsoon circulation is overestimated over South Asia but underestimated over East Asia, bringing a model bias in our quantitative results of the SASM and EASM intensity adjustments. The uncertainties due to the internal climate variability in the model should also not be ignored although we have tried to narrow the uncertainties by conducting an ensemble of ten stochastically perturbed simulations. These limitations indicate that the variational range of the simulated responses of the SASM and EASM duration and intensity presented here should be interpreted with caution. More climate projections for the response scales of the SASM and EASM duration and intensity under different aerosol emission pathways are needed in the future, but our simulations do suggest that a more comprehensive understanding of the impacts of aerosols on the monsoon systems can be achieved by separating aerosol absorbing and scattering components.

https://doi.org/10.5194/egusphere-2023-407
Preprint. Discussion started: 28 March 2023

Numerical experiments are conducted by implementing the same level of reductions in the emissions of SCT, ABS and total aerosol. The summer climate adjustments over Asia are controlled by the impacts of the SCT, although are counterbalanced by the opposite changes induced by the ABS to some extent. The relative weaker response of the direct radiative forcing to the evolution of BC emissions has been reported by Ocko et al. (2014) based on a coupled atmosphere-ocean National Oceanic and Atmospheric Administration Geophysical Fluid Dynamics Laboratory global climate model. Liu et al. (2009) also pointed out that the forcing from BC aerosols over Asia is relatively weak and limited. Our findings indicate that the SCT reduction will bring greater changes in Asian monsoon if the same emission control is implemented on the SCT and ABS aerosols. It is plausible that aerosol-cloud-interactions force some of this response; a reduction in SCT by 75% (mainly from sulfate and organic aerosols) will lead to a greater reduction in cloud-condensation nuclei than a reduction in absorbing aerosols by 75% (mainly from BC). While our work implicitly contains these impacts, future work should examine the attribution between aerosol-radiation interactions and aerosol-cloud-interactions.

In addition, the slow climate feedback associated with the SST under the reduction of aerosol emissions cannot be represented in the simulation results due to the short simulation time conducted in this study. Wang et al. (2019) examined the fast and slow responses of Asian monsoon to anthropogenic aerosol forcings and found similar responses of the SASM and EASM to increasing total aerosols, manifesting as a robust drying trend and weakened monsoon circulation. However, they pointed out that the SASM adjustments are dominated by the SST change, while the EASM adjustments are largely due to the fast direct atmospheric response to aerosol radiative forcing. Therefore, we may infer that the long-term adjustments of the SASM and EASM caused by the emission reductions in total aerosols will still be similar, presenting by the enhanced monsoon circulation and increased precipitation, although the dominant mechanisms in regulating the SASM and EASM may be different.

Code and data availability. The observational precipitation data from the Climate Prediction Center (CPC) unified gauge-based daily observations (Chen et al. 2008) and the Global Precipitation Climatology Project (GPCP) rain gauge-satellite combined precipitation dataset (Huffman and Bolvin, 2013) used in this study can be obtained from https://psl.noaa.gov/data/gridded/data.cpc.globalprecip.html (last access: 2nd Jan. 2022) and https://www.ncei.noaa.gov/data/global-precipitation-climatology-project-gpcp-daily/access/ (last access: 15th Feb. 2022), respectively. The precipitation and wind fields from the ECMWF's (European Center for Medium-Range Weather Forecast) Fifth-generation Reanalysis (ERA5; Hersbach et al., 2020) are available at https://cds.climate.copernicus.eu/cdsapp#!/search?type=dataset&text=ERA5 (last access: 15th Feb. 2022). The CMIP6 historical simulations of the UKESM1 model are available at https://esgf-node.llnl.gov/search/cmip6/ (last access: 11th Feb. 2022). The model outputs and codes can be accessed by contacting Chenwei Fang via fangcw515@163.com.

Author contributions. The majority of this work was completed when CF was visiting the University of Exeter in the UK under

https://doi.org/10.5194/egusphere-2023-407
Preprint. Discussion started: 28 March 2023

the scholarship from China Scholarship Council. JMH proposed the idea. He also supervised this work and revised the manuscript together with JL. BTJ performed the UKESM1 simulations. JL, YC and BZ provided useful suggestions for the study. All authors made contributions to the writing of this study.

Competing interests. The authors declare that they have no conflict of interest.

Acknowledgments. We are grateful to the University of Exeter for providing the academic platform for this study and Met Office for doing the numerical calculations in this work.

Financial support. This work is financially supported by the National Natural Science Foundation of China (42021004, 42192512). JMH and JL would like to acknowledge support from the NERC funded SASSO standard grant (NE/ S00212X/1).

References

Archibald, A. T., O'Connor, F. M., Abraham, N. L., Archer-Nicholls, S., Chipperfield, M. P., Dalvi, M., Folberth, G. A., Dennison, F., Dhomse, S. S., Griffiths, P. T., Hardacre, C., Hewitt, A. J., Hill, R. S., Johnson, C. E., Keeble, J., Köhler, M. O., Morgenstern, O., Mulcahy, J. P., Ordóñez, C., Pope, R. J., Rumbold, S. T., Russo, M. R., Savage, N. H., Sellar, A., Stringer, M., Turnock, S. T., Wild, O. and Zeng, G.: Description and evaluation of the UKCA stratosphere-troposphere chemistry scheme (StratTrop vn 1.0) implemented in UKESM1, Geosci. Model Dev., 13(3), 1223-1266, doi:10.5194/gmd-13-1223-2020, 2020.

Bellouin, N., Mann, G. W., Woodhouse, M. T., Johnson, C., Carslaw, K. S., and Dalvi, M.: Impact of the modal aerosol scheme GLOMAP-mode on aerosol forcing in the Hadley Centre Global Environmental Model, Atmos. Chem. Phys., 13(6), 3027-3044, doi:10.5194/acp-13-3027-2013, 2013.

Bollasina, M. A., Ming, Y., and Ramaswamy, V.: Anthropogenic Aerosols and the Weakening of the South Asian Summer Monsoon, Science, 334(6055), 502-505, doi:10.1126/science.1204994, 2011.

Bollasina, M. A., Ming, Y., and Ramaswamy, V.: Earlier onset of the Indian monsoon in the late twentieth century: The role of anthropogenic aerosols, Geophys. Res. Lett., 40(14), 3715-3720. doi:10.1002/grl.50719, 2013.

https://doi.org/10.5194/egusphere-2023-407
Preprint. Discussion started: 28 March 2023

Bollasina, M. A., Ming, Y., Ramaswamy, V., Schwarzkopf, M. D., and Naik, V.: Contribution of local and remote anthropogenic aerosols to the twentieth century weakening of the South Asian Monsoon, Geophys. Res. Lett., 41(2), 680-687, doi:10.1002/2013gl058183, 2014.

Cai, X., Li, Y., Kang, Z., and Zhang, X.: Characteristics of South Asia High in Summer in 2010 and Its Relationship with Rainbands in China, J. geosci. environ., 05(07), 210-222, doi:10.4236/gep.2017.57016, 2017.

Chen, M., Shi, W., Xie, P., Silva, V. B. S., Kousky, V. E., Higgins, R. W., and Janowiak, J. E.: Assessing objective techniques for gauge-based analyses of global daily precipitation, J. Geophys. Res. Atmos., 113(D4), doi:10.1029/2007jd009132, 2008.

Chiang, J. C. H., Swenson, L. M., and Kong, W.: Role of seasonal transitions and the westerlies in the interannual variability of the East Asian summer monsoon precipitation, Geophys. Res. Lett., 44(8), 3788-3795, doi:10.1002/2017gl072739, 2017.

Collins, W. J., Bellouin, N., Doutriaux-Boucher, M., Gedney, N., Halloran, P., Hinton, T., Hughes, J., Jones, C. D., Joshi, M., Liddicoat, S., Martin, G., O'Connor, F., Rae, J., Senior, C., Sitch, S., Totterdell, I., Wiltshire, A., and Woodward, S.: Development and evaluation of an Earth-System model-HadGEM2, Geosci. Model Dev., 4(4), 1051-1075, doi:10.5194/gmd-4-1051-2011, 2011.

Cox, S. J., Wang, W.-C., and Schwartz, S. E.: Climate response to radiative forcings by sulfate aerosols and greenhouse gases, Geophys. Res. Lett., 22(18), 2509-2512, doi:10.1029/95gl02477, 1995.

Diao, C., Xu, Y., and Xie, S.-P.: Anthropogenic aerosol effects on tropospheric circulation and sea surface temperature (1980-2020): separating the role of zonally asymmetric forcings, Atmos. Chem. Phys., 21(24), 18499-18518, doi:10.5194/acp-21-18499-2021, 2021.

Dong, B., Sutton, R., Shaffrey, L., and Harvey, B.: Recent decadal weakening of the summer Eurasian westerly jet attributable to anthropogenic aerosol emissions, Nat. Commun., 13(1), 1148, doi:10.5194/egusphere-egu22-9731, 2022.

Fahrenbach, N. L. S., and Bollasina, M. A.: Hemispheric-wide climate response to regional COVID-19-related aerosol emission reductions: the prominent role of atmospheric circulation adjustments, Atmos. Chem. Phys., 23(2), 877-894, doi:10.5194/acp-23-877-2023, 2023.

Fyfe, J. C., Kharin, V. V., Swart, N., Flato, G. M., Sigmond, M., and Gillett, N. P.: Quantifying the influence of short-term emission reductions on climate, Sci. Adv., 7(10), doi:10.1126/sciadv.abf7133, 2021.

Ganguly, D., Rasch, P. J., Wang, H., and Yoon, J.: Fast and slow responses of the South Asian monsoon system to anthropogenic aerosols, Geophys. Res. Lett., 39(18), doi:10.1029/2012gl053043, 2012.

Grandey, B. S., Yeo, L. K., Lee, H., and Wang, C.: The Equilibrium Climate Response to Sulfur Dioxide and Carbonaceous Aerosol Emissions From East and Southeast Asia, Geophys. Res. Lett., 45(20), doi:10.1029/2018gl080127, 2018.

Guo, Q.: The summer monsoon intensity index in East Asia and its variation, Acta Geogr. Sin., 38(3), 207-217, doi:10.11821/xb198303001, 1983 (in Chinese).

Ha, K.-J., Seo, Y.-W., Lee, J.-Y., Kripalani, R. H., and Yun, K.-S.: Linkages between the South and East Asian summer monsoons: a review and revisit, Clim. Dyn., 51(11-12), 4207-4227, doi: 10.1007/s00382-017-3773-z, 2017.

https://doi.org/10.5194/egusphere-2023-407
Preprint. Discussion started: 28 March 2023

He, J. H., Zhao, P., Zhu C. W., Zhang, R. H., Tang, X., Chen, L. X., and Zhou, X. J.: Discussion of some problems as to the East Asian subtropical monsoon, J. Meteorol. Res., 22(4), 419-434, doi:10.1029/2007JD008874, 2008.

He, J. and Zhu, Z.: The relation of South China Sea monsoon onset with the subsequent rainfall over the subtropical East Asia, Int. J. Climatol., 35(15), 4547-4556, doi:10.1002/joc.4305, 2015.

Herbert, R., Wilcox, L. J., Joshi, M., Highwood, E., and Frame, D.: Nonlinear response of Asian summer monsoon precipitation to emission reductions in South and East Asia, Environ. Res. Lett., 17(1), 014005, doi:10.1088/1748-9326/ac3b19, 2021.

Hersbach, H., Bell, B., Berrisford, P., Hirahara, S., Horányi, A., Muñoz-Sabater, J., Nicolas, J., Peubey, C., Radu, R., Schepers, D., Simmons, A., Soci, C., Abdalla, S., Abellan, X., Balsamo, G., Bechtold, P., Biavati, G., Bidlot, J., Bonavita, M., Chiara, G. De, Dahlgren, P., Dee, D., Diamantakis, M., Dragani, R., Flemming, J., Forbes, R., Fuentes, M., Geer, A., Haimberger, L., Healy, S., Hogan, R. J., Hólm, E., Janisková, M., Keeley, S., Laloyaux, P., Lopez, P., Lupu, C., Radnoti, G., Rosnay, P. de, Rozum, I., Vamborg, F., Villaume, S. and Thépaut, J. N.: The ERA5 global reanalysis. Q. J. R. Meteorol. Soc., 146(730), 1999-2049, doi:10.1002/qj.3803, 2020.

Huang, R., Liu, Y., Du, Z., Chen, J., and Huangfu, J.: Differences and links between the East Asian and South Asian summer monsoon systems: Characteristics and Variability, Adv. Atmos. Sci., 34(10), 1204-1218, doi:10.1007/s00376-017-7008-3, 2017.

Huffman, G. J. and Bolvin, D. T.: GPCP version 2.2 SG combined precipitation data set documentation, NASA GSFC Doc., Internet Publication, 1-46, available at https://www.researchgate.net/profile/George-Huffman/publication/228592168_GPCP_version_2_combined_precipitation_data_set_documentation/links/5aff8194aca2720ba095eed8/GPCP-version-2-combined-precipitation-data-set-documentation.pdf, 2013.

Iturbide, M., Gutiérrez, J. M., Alves, L. M., Bedia, J., Cerezo-Mota, R., Cimadevilla, E., Cofiño, A. S., Di Luca, A., Faria, S. H., Gorodetskaya, I. V., Hauser, M., Herrera, S., Hennessy, K., Hewitt, H. T., Jones, R. G., Krakovska, S., Manzanas, R., Martínez-Castro, D., Narisma, G. T., Nurhati, I. S., Pinto, I., Seneviratne, S. I., Hurk, B. van den and Vera, C. S.: An update of IPCC climate reference regions for subcontinental analysis of climate model data: definition and aggregated datasets, Earth Syst. Sci. Data, 12(4), 2959-2970, doi:10.5194/essd-12-2959-2020, 2020.

Ji, Z., Kang, S., Zhang, D., Zhu, C., Wu, J., and Xu, Y.: Simulation of the anthropogenic aerosols over South Asia and their effects on Indian summer monsoon, Clim. Dyn., 36(9-10), 1633-1647, doi:10.1007/s00382-010-0982-0, 2011.

Jiang, Y., Liu, X., Yang, X.-Q., and Wang, M.: A numerical study of the effect of different aerosol types on East Asian summer clouds and precipitation, Atmos. Environ., 70, 51-63, doi:10.1016/j.atmosenv.2012.12.039, 2013.

Khadka, D., Babel, M. S., Abatan, A. A., and Collins, M.: An evaluation of CMIP5 and CMIP6 climate models in simulating summer rainfall in the Southeast Asian monsoon domain, Int. J. Climatol., 42(2), 1181-1202, doi: 10.1002/joc.7296, 2021.

Kloster, S., Dentener, F., Feichter, J., Raes, F., Lohmann, U., Roeckner, E., and Fischer-Bruns, I.: A GCM study of future climate response to aerosol pollution reductions, Clim. Dyn., 34(7-8), 1177-1194, doi:10.1007/s00382-009-0573-0, 2009.

https://doi.org/10.5194/egusphere-2023-407
Preprint. Discussion started: 28 March 2023

Kloster, S., Dentener, F., Feichter, J., Raes, F., van Aardenne, J., Roeckner, E., Lohmann, U., Stier, P., and Swart, R.: Influence of future air pollution mitigation strategies on total aerosol radiative forcing, Atmos. Chem. Phys., 8(21), 6405-6437, doi:10.5194/acp-8-6405-2008, 2008.

Kuhlbrodt, T., Jones, C. G., Sellar, A., Storkey, D., Blockley, E., Stringer, M., Hill, R., Graham, T., Ridley, J., Blaker, A., Calvert, D., Copsey, D., Ellis, R., Hewitt, H., Hyder, P., Ineson, S., Mulcahy, J., Siahaan, A., and Walton, J.: The Low-Resolution Version of HadGEM3 GC3.1: Development and Evaluation for Global Climate, J. Adv. Model. Earth Syst., 10(11), 2865-2888, doi:10.1029/2018ms001370, 2018.

Lal, P., Kumar, A., Kumar, S., Kumari, S., Saikia, P., Dayanandan, A., Adhikari, D., and Khan, M. L.: The dark cloud with a silver lining: Assessing the impact of the SARS COVID-19 pandemic on the global environment, Sci. Total Environ., 732, 139297, doi:10.1016/j.scitotenv.2020.139297, 2020.

Lau, W. K. M., Kim, K.-M., and Ruby Leung, L.: Changing circulation structure and precipitation characteristics in Asian monsoon regions: greenhouse warming vs. aerosol effects, Geosci. Lett., 4(1), doi:10.1186/s40562-017-0094-3, 2017.

Le, T., Wang, Y., Liu, L., Yang, J., Yung, Y. L., Li, G., and Seinfeld, J. H.: Unexpected air pollution with marked emission reductions during the COVID-19 outbreak in China, Science, 369(6504), 702-706, doi:10.1126/science.abb7431, 2020.

Li, C., McLinden, C., Fioletov, V., Krotkov, N., Carn, S., Joiner, J., Streets, D., He, H., Ren, X., Li, Z., and Dickerson, R. R.: India Is Overtaking China as the World's Largest Emitter of Anthropogenic Sulfur Dioxide, Sci. Rep., 7(1), doi:10.1038/s41598-017-14639-8, 2017.

Li, H., Yang, Y., Wang, H., Wang, P., Yue, X., and Liao, H.: Projected Aerosol Changes Driven by Emissions and Climate Change Using a Machine Learning Method, Environ. Sci. Technol., 56(7), 3884-3893, doi:10.1021/acs.est.1c04380, 2022.

Li, J., Carlson, B. E., Yung, Y. L., Lv, D., Hansen, J., Penner, J. E., Liao, H., Ramaswamy, V., Kahn, R. A., Zhang, P., Dubovik, O., Ding, A., Lacis, A. A., Zhang, L., and Dong, Y.: Scattering and absorbing aerosols in the climate system, Nat. Rev. Earth Environ., 3(6), 363-379, doi:10.1038/s43017-022-00296-7, 2022.

Li, L., Li, Q., Huang, L., Wang, Q., Zhu, A., Xu, J., Liu, Z., Li, H., Shi, L., Li, R., Azari, M., Wang, Y., Zhang, X., Liu, Z., Zhu, Y., Zhang, K., Xue, S., Ooi, M. C. G., Zhang, D., and Chan, A.: Air quality changes during the COVID-19 lockdown over the Yangtze River Delta Region: An insight into the impact of human activity pattern changes on air pollution variation, Sci. Total Environ., 732, 139282, doi:10.1016/j.scitotenv.2020.139282, 2020.

Li, X., Ting, M., and Lee, D. E.: Fast Adjustments of the Asian Summer Monsoon to Anthropogenic Aerosols, Geophys. Res. Lett., 45(2), 1001-1010, doi:10.1002/2017gl076667, 2018.

Li, Z., Lau, W. K. -M., Ramanathan, V., Wu, G., Ding, Y., Manoj, M. G., Liu, J., Qian, Y., Li, J., Zhou, T., Fan, J., Rosenfeld, D., Ming, Y., Wang, Y., Huang, J., Wang, B., Xu, X., Lee, S. -S., Cribb, M., Zhang, F., Yang, X., Zhao, C., Takemura, T., Wang, K., Xia, X., Yin, Y., Zhang, H., Guo, J., Zhai, P. M., Sugimoto, N., Babu, S. S. and Brasseur G. P.: Aerosol and monsoon climate interactions over Asia, Rev. Geophys., 54(4), 866-929, doi:10.1002/2015rg000500, 2016.

Liepert, B. G., Feichter, J., Lohmann, U., and Roeckner, E.: Can aerosols spin down the water cycle in a warmer and moister world? Geophys. Res. Lett., 31(6), doi:10.1029/2003gl019060, 2004.

https://doi.org/10.5194/egusphere-2023-407
Preprint. Discussion started: 28 March 2023

Liu, Y., Sun, J., and Yang, B.: The effects of black carbon and sulphate aerosols in China regions on East Asia monsoons, Tellus B: Chem. Phys. Meteorol., 61(4), doi:10.3402/tellusb.v61i4.16861, 2009.

Liu, Z., Ciais, P., Deng, Z., Lei, R., Davis, S. J., Feng, S., Zheng, B., Cui, D., Dou, X., Zhu, B., Guo, R., Ke, P., Sun, T., Lu, C., He, P., Wang, Y., Yue, X., Wang, Y., Lei, Y., Zhou H., Cai, Z., Wu, Y., Guo, R., Han, T., Xue, J., Boucher, O., Boucher, E., Chevallier, F., Tanaka, K., Wei, Y., Zhong, H., Kang, C., Zhang, N., Chen, B., Xi, F., Liu, M., Bréon, F. M., Lu, Y., Zhang, Q., Guan, D., Gong, P., Kammen, D. M., He, K., and Schellnhuber, H. J.: Near-real-time monitoring of global CO_2 emissions reveals the effects of the COVID-19 pandemic, Nat. Commun., 11(1), doi:10.1038/s41467-020-18922-7, 2020.

Lund, M. T., Myhre, G., and Samset, B. H.: Anthropogenic aerosol forcing under the Shared Socioeconomic Pathways, Atmos. Chem. Phys., 19(22), 13827-13839, doi:10.5194/acp-19-13827-2019, 2019.

Madhu, V.: Variation of Zonal Winds in the Upper Troposphere and Lower Stratosphere in Association with Deficient and Excess Indian Summer Monsoon Scenario, Atmos. Clim. Sci., 04(04), 685-695, doi:10.4236/acs.2014.44062, 2014.

Mann, G. W., Carslaw, K. S., Spracklen, D. V., Ridley, D. A., Manktelow, P. T., Chipperfield, M. P., Pickering, S. J., and Johnson, C. E.: Description and evaluation of GLOMAP-mode: a modal global aerosol microphysics model for the UKCA composition-climate model, Geosci. Model Dev., 3(2), 519-551, doi:10.5194/gmd-3-519-2010, 2010.

Meinshausen, M., Nicholls, Z. R. J., Lewis, J., Gidden, M. J., Vogel, E., Freund, M., Beyerle, U., Gessner, C., Nauels, A., Bauer, N., Canadell, J. G., Daniel, J. S., John, A., Krummel, P. B., Luderer, G., Meinshausen, N., Montzka, S. A., Rayner, P. J., Reimann, S., Smith, S. J., Berg, M. van den, Velders, G. J. M., Vollmer, M. K., and Wang, R. H. J.: The shared socio-economic pathway (SSP) greenhouse gas concentrations and their extensions to 2500, Geosci. Model Dev., 13(8), 3571-3605, doi:10.5194/gmd-13-3571-2020, 2020.

Menon, S., Hansen, J., Nazarenko, L., and Luo, Y.: Climate Effects of Black Carbon Aerosols in China and India, Science, 297(5590), 2250-2253, doi:10.1126/science.1075159, 2002.

Mishra, V., Smoliak, B. V., Lettenmaier, D. P., and Wallace, J. M.: A prominent pattern of year-to-year variability in Indian Summer Monsoon Rainfall, Proc. Natl. Acad. Sci. U.S.A., 109(19), 7213-7217, doi:10.1073/pnas.1119150109, 2012.

Morgenstern, O., Braesicke, P., O'Connor, F. M., Bushell, A. C., Johnson, C. E., Osprey, S. M., and Pyle, J. A.: Evaluation of the new UKCA climate-composition model-Part 1: The stratosphere, Geosci. Model Dev., 2(1), 43-57, doi:10.5194/gmd-2-43-2009, 2009.

Morgenstern, O., Hegglin, M. I., Rozanov, E., O'Connor, F. M., Abraham, N. L., Akiyoshi, H., Archibald, A. T., Bekki, S., Butchart, N., Chipperfield, M. P., Deushi, M., Dhomse, S. S., Garcia, R. R., Hardiman, S. C., Horowitz, L. W., Jöckel, P., Josse, B., Kinnison, D., Lin, M., Mancini, E., Manyin, M. E., Marchand, M., Marécal, V., Michou, M., Oman, L. D., Pitari, G., Plummer, D. A., Revell, L. E., Saint-Martin, D., Schofield, R., Stenke, A., Stone, K., Sudo, K., Tanaka, T. Y., Tilmes, S., Yamashita, Y., Yoshida, K., and Zeng, G.: Review of the global models used within phase 1 of the Chemistry-Climate Model Initiative (CCMI), Geosci. Model Dev., 10(2), 639-671, doi:10.5194/gmd-10-639-2017, 2017.

https://doi.org/10.5194/egusphere-2023-407
Preprint. Discussion started: 28 March 2023

Mulcahy, J. P., Jones, C., Sellar, A., Johnson, B., Boutle, I. A., Jones, A., Andrews, T., Rumbold, S. T., Mollard, J., Bellouin, N., Johnson, C. E., Williams, K. D., Grosvenor, D. P., and McCoy, D. T.: Improved Aerosol Processes and Effective Radiative Forcing in HadGEM3 and UKESM1, J. Adv. Model. Earth Syst., 10(11), 2786-2805, doi:10.1029/2018ms001464, 2018.

Noska, R. and Misra, V.: Characterizing the onset and demise of the Indian summer monsoon, Geophys. Res. Lett., 43(9), 4547-4554, doi:10.1002/2016gl068409, 2016.

O'Connor, F. M., Abraham, N. L., Dalvi, M., Folberth, G. A., Griffiths, P. T., Hardacre, C., Johnson, B. T., Kahana, R., Keeble, J., Kim, B., Morgenstern, O., Mulcahy, J. P., Richardson, M., Robertson, E., Seo, J., Shim, S., Teixeira, J. C., Turnock, S. T., Williams, J., Wiltshire, A. J., Woodward, S., and Zeng, G.: Assessment of pre-industrial to present-day anthropogenic climate forcing in UKESM1, Atmos. Chem. Phys., 21(2), 1211-1243, doi:10.5194/acp-21-1211-2021, 2021.

O'Connor, F. M., Johnson, C. E., Morgenstern, O., Abraham, N. L., Braesicke, P., Dalvi, M., Folberth, G. A., Sanderson, M. G., Telford, P. J., Voulgarakis, A., Young, P. J., Zeng, G., Collins, W. J., and Pyle, J. A.: Evaluation of the new UKCA climate-composition model-Part 2: The Troposphere, Geosci. Model Dev., 7(1), 41-91, doi:10.5194/gmd-7-41-2014, 2014.

Ocko, I. B., Ramaswamy, V., and Ming, Y.: Contrasting Climate Responses to the Scattering and Absorbing Features of Anthropogenic Aerosol Forcings, J. Clim., 27(14), 5329-5345, doi:10.1175/jcli-d-13-00401.1, 2014.

Persad, G. G., Samset, B. H., and Wilcox, L. J.: Aerosols must be included in climate risk assessments, Nature, 611(7937), 662-664, doi:10.1038/d41586-022-03763-9, 2022.

Rao, S., Klimont, Z., Smith, S. J., Van Dingenen, R., Dentener, F., Bouwman, L., Riahi, K., Amann, M., Bodirsky, B. L., van Vuuren, D. P., Aleluia Reis, L., Calvin, K., Drouet, L., Fricko, O., Fujimori, S., Gernaat, D., Havlik, P., Harmsen, M., Hasegawa, T., Heyes, C., Hilaire, J., Luderer, G., Masui, T., Stehfest, E., Strefler, J., Sluis, S. van der, and Tavoni, M.: Future air pollution in the Shared Socio-economic Pathways, Glob. Environ. Change, 42, 346-358, doi:10.1016/j.gloenvcha.2016.05.012, 2017.

Rosenfeld, D., Dai, J., Yu, X., Yao, Z., Xu, X., Yang, X., and Du, C., Inverse Relations Between Amounts of Air Pollution and Orographic Precipitation, Science, 315(5817), 1396-1398, doi:10.1126/science.1137949, 2007.

Salzmann, M., Weser, H., and Cherian, R.: Robust response of Asian summer monsoon to anthropogenic aerosols in CMIP5 models, J. Geophys. Res. Atmos., 119(19), 11,321-11,337, doi:10.1002/2014jd021783, 2014.

Samset, B. H., Sand, M., Smith, C. J., Bauer, S. E., Forster, P. M., Fuglestvedt, J. S., Osprey, S., and Schleussner, C. -F.: Climate Impacts From a Removal of Anthropogenic Aerosol Emissions, Geophys. Res. Lett., 45(2), 1020-1029, doi:10.1002/2017gl076079, 2018.

Sellar, A. A., Jones, C. G., Mulcahy, J. P., Tang, Y., Yool, A., Wiltshire, A., O'Connor, F. M., Stringer, M., Hill, R., Palmieri, J., Woodward, S., Mora, L., Kuhlbrodt, T., Rumbold, S. T., Kelley, D. I., Ellis, R., Johnson, C. E., Walton, J., Abraham, N. L., Andrews, M. B., Andrews, T., Archibald, A. T., Berthou, S., Burke, E., Blockley, E., Carslaw, K., Dalvi, M., Edwards, J., Folberth, G. A., Gedney, N., Griffiths, P. T., Harper, A. B., Hendry, M. A., Hewitt, A. J., Johnson, B., Jones, A., Jones, C. D., Keeble, J., Liddicoat, S., Morgenstern, O., Parker, R. J., Predoi, V., Robertson, E., Siahaan, A., Smith, R. S., Swaminathan,

https://doi.org/10.5194/egusphere-2023-407
Preprint. Discussion started: 28 March 2023

R., Woodhouse, M. T., Zeng, G., and Zerroukat, M.: UKESM1: Description and Evaluation of the U.K. Earth System Model, J. Adv. Model. Earth Syst., 11(12), 4513-4558, doi:10.1029/2019ms001739, 2019.

Song, F., Zhou, T., and Qian, Y.: Responses of East Asian summer monsoon to natural and anthropogenic forcings in the 17 latest CMIP5 models, Geophys. Res. Lett., 41(2), 596-603, doi:10.1002/2013gl058705, 2014.

Stohl, A., Aamaas, B., Amann, M., Baker, L. H., Bellouin, N., Berntsen, T. K., Boucher, O., Cherian, R., Collins, W., Daskalakis, N., Dusinska, M., Eckhardt, S., Fuglestvedt, J. S., Harju, M., Heyes, C., Hodnebrog, Ø., Hao, J., Im, U., Kanakidou, M., Klimont, Z., Kupiainen, K., Law, K. S., Lund, M. T., Maas, R., MacIntosh, C. R., Myhre, G., Myriokefalitakis, S., Olivié, D., Quaas, J., Quennehen, B., Raut, J.-C., Rumbold, S. T., Samset, B. H., Schulz, M., Seland, Ø., Shine, K. P., Skeie, R. B., Wang, S., Yttri, K. E., and Zhu, T.: Evaluating the climate and air quality impacts of short-lived pollutants, Atmos. Chem. Phys., 15(18), 10529-10566, doi:10.5194/acp-15-10529-2015, 2015.

Sun, Y. and Ding, Y.: Responses of South and East Asian summer monsoons to different land-sea temperature increases under a warming scenario, Chin. Sci. Bull., 56(25), 2718-2726, doi:10.1007/s11434-011-4602-0, 2011.

Taylor, K. E. and Penner, J. E.: Response of the climate system to atmospheric aerosols and greenhouse gases, Nature, 369(6483), 734-737, doi:10.1038/369734a0, 1994.

Turner, A. G. and Annamalai, H.: Climate change and the South Asian summer monsoon, Nat. Clim. Change, 2(8), 587-595, doi:10.1038/nclimate1495, 2012.

Undorf, S., Polson, D., Bollasina, M. A., Ming, Y., Schurer, A., and Hegerl, G. C.: Detectable Impact of Local and Remote Anthropogenic Aerosols on the 20th Century Changes of West African and South Asian Monsoon Precipitation, J. Geophys. Res. Atmos., 123(10), 4871-4889, doi:10.1029/2017jd027711, 2018.

Vissa, N. K., Satyanarayana, A. N. V., and Prasad Kumar, B.: Intensity of tropical cyclones during pre- and post-monsoon seasons in relation to accumulated tropical cyclone heat potential over Bay of Bengal, Nat. Hazards, 68(2), 351-371, doi:10.1007/s11069-013-0625-y, 2013.

Wang, B., Ding, Q., and Joseph, P. V.: Objective Definition of the Indian Summer Monsoon Onset*, J. Clim., 22(12), 3303-3316, doi:10.1175/2008jcli2675.1, 2009.

Wang, D., Li, X., Tao, W.-K., and Wang, Y.: Effects of vertical wind shear on convective development during a landfall of severe tropical storm Bilis (2006), Atmos. Res., 94(2), 270-275, doi:10.1016/j.atmosres.2009.06.004, 2009.

Wang, D., Zhu, B., Jiang, Z., Yang, X.-Q., and Zhu, T.: The impact of the direct effects of sulfate and black carbon aerosols on the subseasonal march of the East Asian subtropical summer monsoon, J. Geophys. Res. Atmos., 121(6), 2610-2625, doi:10.1002/2015jd024574, 2016.

Wang, H., Xie, S.-P., Kosaka, Y., Liu, Q., and Du, Y.: Dynamics of Asian Summer Monsoon Response to Anthropogenic Aerosol Forcing, J. Clim., 32(3), 843-858, doi:10.1175/jcli-d-18-0386.1, 2019.

Wang, L., Guo, S., and Ge, J.: The timing of the South-Asian High establishment and its relation to tropical Asian summer monsoon and precipitation over east-central China in summer, J. Trop. Meteorol. , 22(2), 136-144, doi:10.16555/j.1006-8775.2016.02.004, 2016.

https://doi.org/10.5194/egusphere-2023-407
Preprint. Discussion started: 28 March 2023

Wang, R., Tao, S., Wang, W., Liu, J., Shen, H., Shen, G., Wang, B., Liu, X., Li, W., Huang, Y., Zhang, Y., Lu, Y., Chen, H., Chen, Y., Wang, C., Zhu, D., Wang, X., Li, B., Liu, W., and Ma, J.: Black Carbon Emissions in China from 1949 to 2050, Environ. Sci. Technol., 46(14), 7595-7603, doi:10.1021/es3003684, 2012.

Wang, Z., Lin, L., Yang, M., and Xu, Y.: The effect of future reduction in aerosol emissions on climate extremes in China, Clim. Dyn., 47(9-10), 2885-2899, doi:10.1007/s00382-016-3003-0, 2016.

Wang, Z., Wang, Q., and Zhang, H.: Equilibrium climate response of the East Asian summer monsoon to forcing of anthropogenic aerosol species, J. Meteorol. Res., 31(6), 1018-1033, doi:10.1007/s13351-017-7059-5, 2017.

Wei, W. and Yang, S.: Interaction between South Asian high and Indian Summer Monsoon rainfall, Indian Summer Monsoon Variability, Elsevier, 319-334, doi:10.1016/b978-0-12-822402-1.00016-8, 2021.

Wei, W., Zhang, R., Wen, M., and Yang, S.: Relationship between the Asian Westerly Jet Stream and Summer Rainfall over Central Asia and North China: Roles of the Indian Monsoon and the South Asian High, J. Clim., 30(2), 537-552, doi:10.1175/jcli-d-15-0814.1, 2017.

Wei, W., Zhang, R., Wen, M., Kim, B.-J., and Nam, J.-C.: Interannual Variation of the South Asian High and Its Relation with Indian and East Asian Summer Monsoon Rainfall, J. Clim., 28(7), 2623-2634, doi:10.1175/jcli-d-14-00454.1, 2015.

West, R. E. L., Stier, P., Jones, A., Johnson, C. E., Mann, G. W., Bellouin, N., Partridge, D. G., and Kipling, Z., The importance of vertical velocity variability for estimates of the indirect aerosol effects, Atmos. Chem. Phys., 14(12), 6369-6393, doi:10.5194/acp-14-6369-2014, 2014.

Westervelt, D. M., Conley, A. J., Fiore, A. M., Lamarque, J.-F., Shindell, D. T., Previdi, M., Mascioli, N. R., Faluvegi, G., Correa, G., and Horowitz, L. W., Connecting regional aerosol emissions reductions to local and remote precipitation responses, Atmos. Chem. Phys., 18(16), 12461-12475, doi:10.5194/acp-18-12461-2018, 2018.

Wilcox, L. J., Liu, Z., Samset, B. H., Hawkins, E., Lund, M. T., Nordling, K., Undorf, S., Bollasina, M., Ekman, A. M. L., Krishnan, S., Merikanto, J., and Turner, A. G.: Accelerated increases in global and Asian summer monsoon precipitation from future aerosol reductions, Atmos. Chem. Phys., 20(20), 11955-11977, doi:10.5194/acp-20-11955-2020, 2020.

Williams, K. D., Copsey, D., Blockley, E. W., Bodas-Salcedo, A., Calvert, D., Comer, R., Davis, P., Graham, T., Hewitt, H. T., Hill, R., Hyder, P., Ineson, S., Johns, T. C., Keen, A. B., Lee, R. W., Megann, A., Milton, S. F., Rae, J. G. L., Roberts, M. J., Scaife, A. A., Schiemann, R., Storkey, D., Thorpe, L., Watterson, I. G., Walters, D. N., West, A., Wood, R. A., Woollings, T., and Xavier, P. K.: The Met Office Global Coupled Model 3.0 and 3.1 (GC3.0 and GC3.1) Configurations, J. Adv. Model. Earth Syst., 10(2), 357-380, doi:10.1002/2017ms001115, 2018.

Woodward, S.: Modeling the atmospheric life cycle and radiative impact of mineral dust in the Hadley Centre climate model, J. Geophys. Res. Atmos., 106(D16), 18155-18166, doi:10.1029/2000jd900795, 2001.

Xie, Z., Du, Y., and Yang, S.: Zonal Extension and Retraction of the Subtropical Westerly Jet Stream and Evolution of Precipitation over East Asia and the Western Pacific, J. Clim., 28(17), 6783-6798, doi:10.1175/jcli-d-14-00649.1, 2015.

Xin, X., Wu, T., Zhang, J., Yao, J., and Fang, Y.: Comparison of CMIP6 And CMIP5 simulations of precipitation in China and the East Asian summer monsoon, Int. J. Climatol., 40(15), 6423-6440, doi:10.1002/joc.6590, 2020.

https://doi.org/10.5194/egusphere-2023-407
Preprint. Discussion started: 28 March 2023

Xing, J., Wang, J., Mathur, R., Pleim, J., Wang, S., Hogrefe, C., Gan, C.-M., Wong, D. C., and Hao, J.: Unexpected Benefits of Reducing Aerosol Cooling Effects, Environ. Sci. Technol., 50(14), 7527-7534, doi:10.1021/acs.est.6b00767, 2016.

Yang, Y., Ren, L., Li, H., Wang, H., Wang, P., Chen, L., Yue, X., and Liao, H.: Fast Climate Responses to Aerosol Emission Reductions During the COVID-19 Pandemic, Geophys. Res. Lett., 47(19), doi:10.1029/2020gl089788, 2020.

Yu, X., Zhang, L., Zhou, T., and Liu, J.: The Asian Subtropical Westerly Jet Stream in CRA-40, ERA5, and CFSR Reanalysis Data: Comparative Assessment, J. Meteorol. Res., 35(1), 46-63, doi:10.1007/s13351-021-0107-1, 2021.

Zeng, Q., Zhang, Y., Lei, H., Xie, Y., Gao, T., Zhang, L., Wang, C., and Huang, Y.: Microphysical Characteristics of Precipitation during Pre-monsoon, Monsoon, and Post-monsoon Periods over the South China Sea, Adv. Atmos. Sci., 36(10), 1103-1120, doi:10.1007/s00376-019-8225-8, 2019.

Zhao, A. D., Stevenson, D. S., and Bollasina, M. A., The role of anthropogenic aerosols in future precipitation extremes over the Asian Monsoon Region, Clim. Dyn., 52(9-10), 6257-6278, doi:10.1007/s00382-018-4514-7, 2018.

Zhao, P., Zhang, R., Liu, J., Zhou, X., and He, J.: Onset of southwesterly wind over eastern China and associated atmospheric circulation and rainfall, Clim. Dyn., 28(7-8), 797-811, doi:10.1007/s00382-006-0212-y, 2006.

Zheng, B., Tong, D., Li, M., Liu, F., Hong, C., Geng, G., Li, H., Li, X., Peng, L., Qi, J., Yan, L., Zhang, Y., Zhao, H., Zheng, Y., He, K., and Zhang, Q.: Trends in China's anthropogenic emissions since 2010 as the consequence of clean air actions, Atmos. Chem. Phys., 18(19), 14095-14111, doi:10.5194/acp-18-14095-2018, 2018.

Zhou, X., Chen, F., Wu, X., Qian, R., Liu, X., and Wang, S.: Variation Characteristics of Stable Isotopes in Precipitation and Response to Regional Climate Conditions during Pre-monsoon, Monsoon and Post-monsoon Periods in the Tianshui Area, Water, 12(9), 2391, doi:10.3390/w12092391, 2020.

https://doi.org/10.5194/egusphere-2023-407
Preprint. Discussion started: 28 March 2023

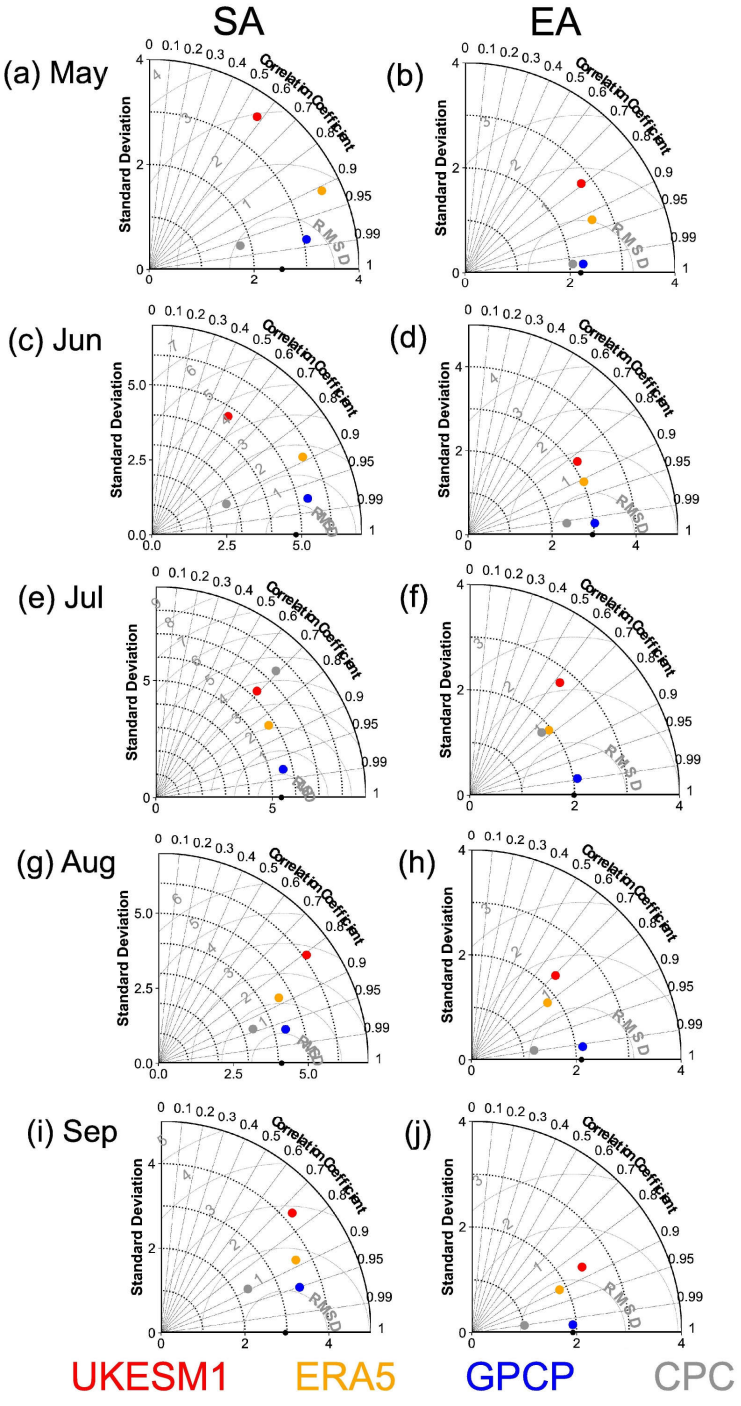

Figure 1: Taylor diagrams for the simulated climatological monthly mean (1985-2014) summer precipitation (unit: mm day^{-1}) over South Asia (a, c, e, g and i) and East Asia (b, d, f, h and j) from the CMIP6-UKESM1 historical simulation (red dots), ERA5 reanalysis (yellow dots), GPCP dataset (blue dots) and CPC observations (gray dots). The merged observed mean values of the GPCP and CPC datasets are shown as black dots. The angular co-ordinate gives the correlation with the mean values of observations. The radial co-ordinate gives the standard deviations of different datasets. The dotted gray lines represent the root-mean-square deviation (RMSD).

https://doi.org/10.5194/egusphere-2023-407
Preprint. Discussion started: 28 March 2023

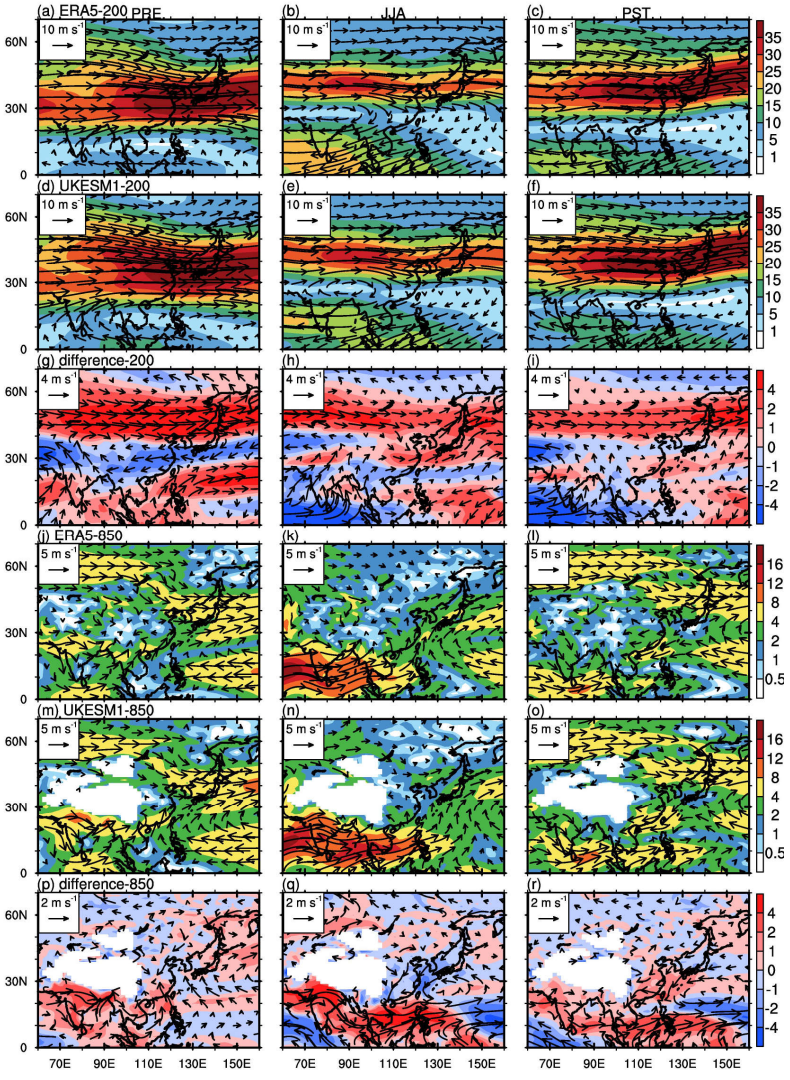

740 **Figure 2: Spatial distributions of the climatological mean (1985-2014) wind directions (vectors; unit: m s^{-1}) and wind speeds (shading; unit: m s^{-1}) at 200 hPa (a-i) and 850 hPa (j-r) from ERA5 reanalysis (a-c and j-l) and CMIP6-UKESM1 historical simulation (d-f and m-o) over Asia during pre-monsoon (April-May; a, d, g, j, m and p), monsoon (June-August; b, e, h, k, n and g) and post-monsoon (September-October; c, f, i, l, o and r) seasons. Panels (g-i) and (p-r) show the differences between the wind fields from the UKESM1 simulation and ERA5 reanalysis at 200 hPa and 850 hPa, respectively.**

https://doi.org/10.5194/egusphere-2023-407
Preprint. Discussion started: 28 March 2023

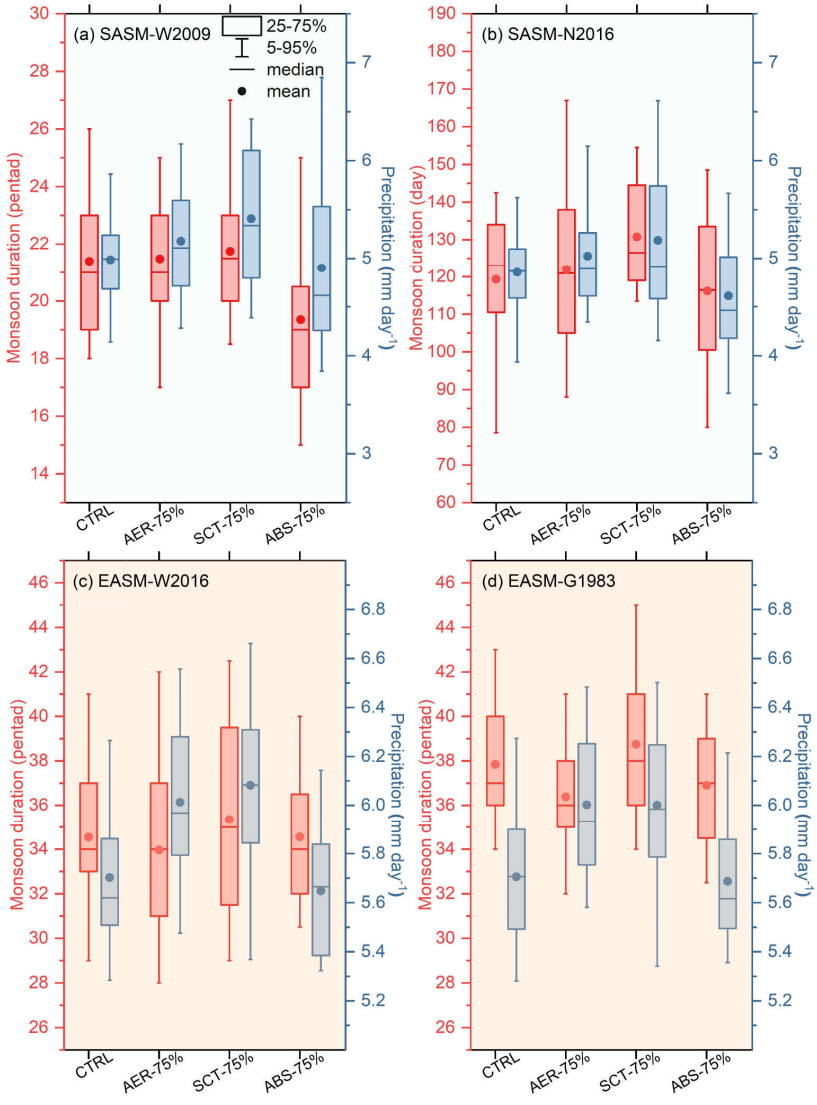

Figure 3: Box diagrams of the monsoon duration (red; unit: pentad for a, c and d, day for b) and precipitation (blue; unit: mm day^{-1}) over South Asia (a and b) and East Asia (c and d) in different simulations. Dots and middle horizontal lines inside boxes indicate mean and median values, respectively, and lower and upper sides of boxes indicate 25 and 75% range, respectively, and top and bottom line represent 5% and 95%, respectively. Panel (a) is derived based on the definition from Wang et al. (2009; hereafter referred to as W2009). Panel (b) is derived based on the definition from Noska and Misra (2016; hereafter referred to as N2016). Panel (c) is derived based on the definition from Wang, D. et al (2016; hereafter referred to as W2016). Panel (d) is derived based on the definition from Guo (1983; hereafter referred to as G1983).

https://doi.org/10.5194/egusphere-2023-407
Preprint. Discussion started: 28 March 2023

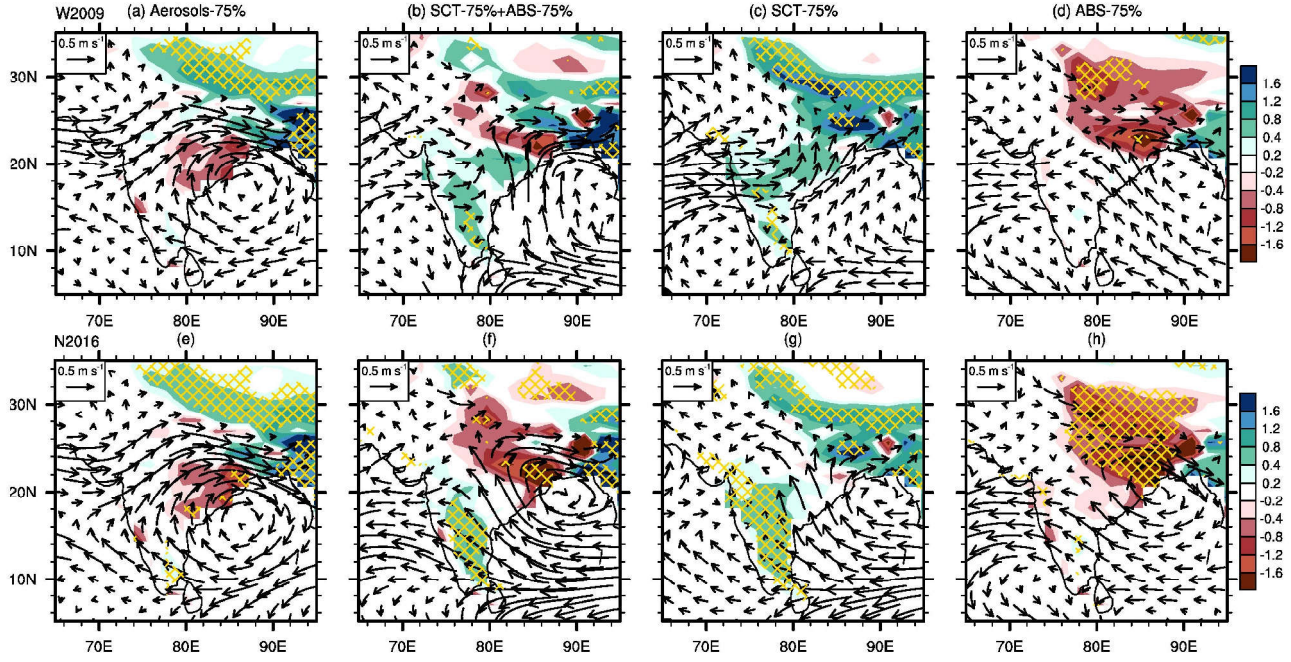

Figure 4: Spatial distributions of the monsoon precipitation (shading; unit: mm day-1) and 850-hPa wind fields (vector; unit: m s^{-1}) responses to the reductions in total aerosols (a and e), scattering aerosols (SCT; c and g) and absorbing aerosols (ABS; d and h) over South Asia. Panels (b) and (f) are the linear addition of the impacts of the reductions in the SCT and ABS. Hatched regions denote where the precipitation change is statistically significant at the 95% confidence level according to a Wilcoxon rank sum test. Panels (a)-(d) are derived based on the definition from W2009. Panels (e)-(h) are derived based on the definition from N2016.

https://doi.org/10.5194/egusphere-2023-407
Preprint. Discussion started: 28 March 2023

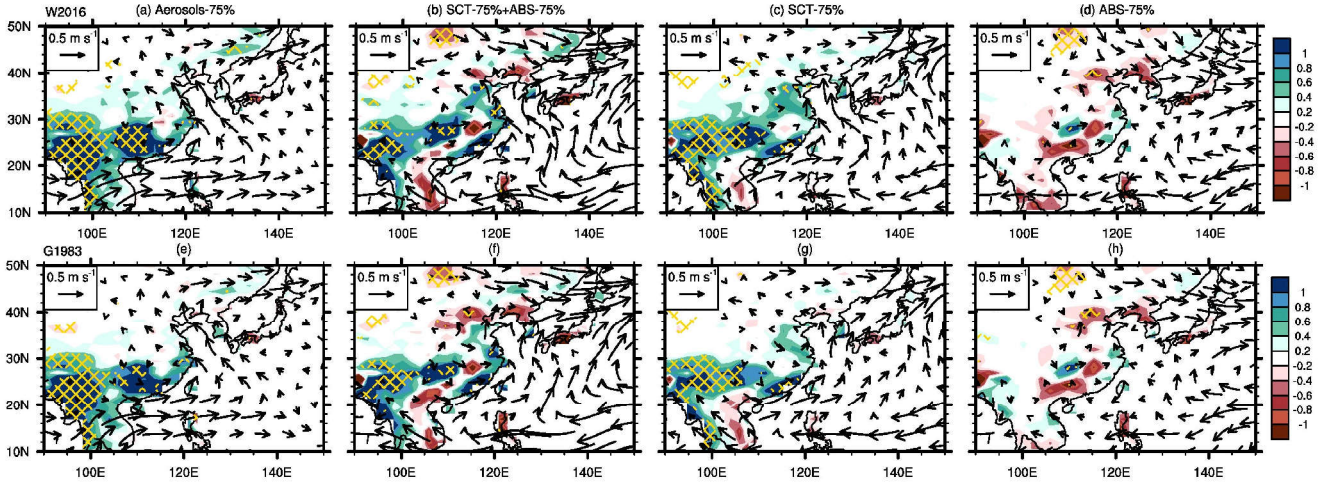

765

Figure 5: Same as Figure 4, but for East Asia. Panels (a)-(d) are derived based on the definition from W2016. Panels (e)-(h) are derived based on the definition from G1983.

https://doi.org/10.5194/egusphere-2023-407
Preprint. Discussion started: 28 March 2023

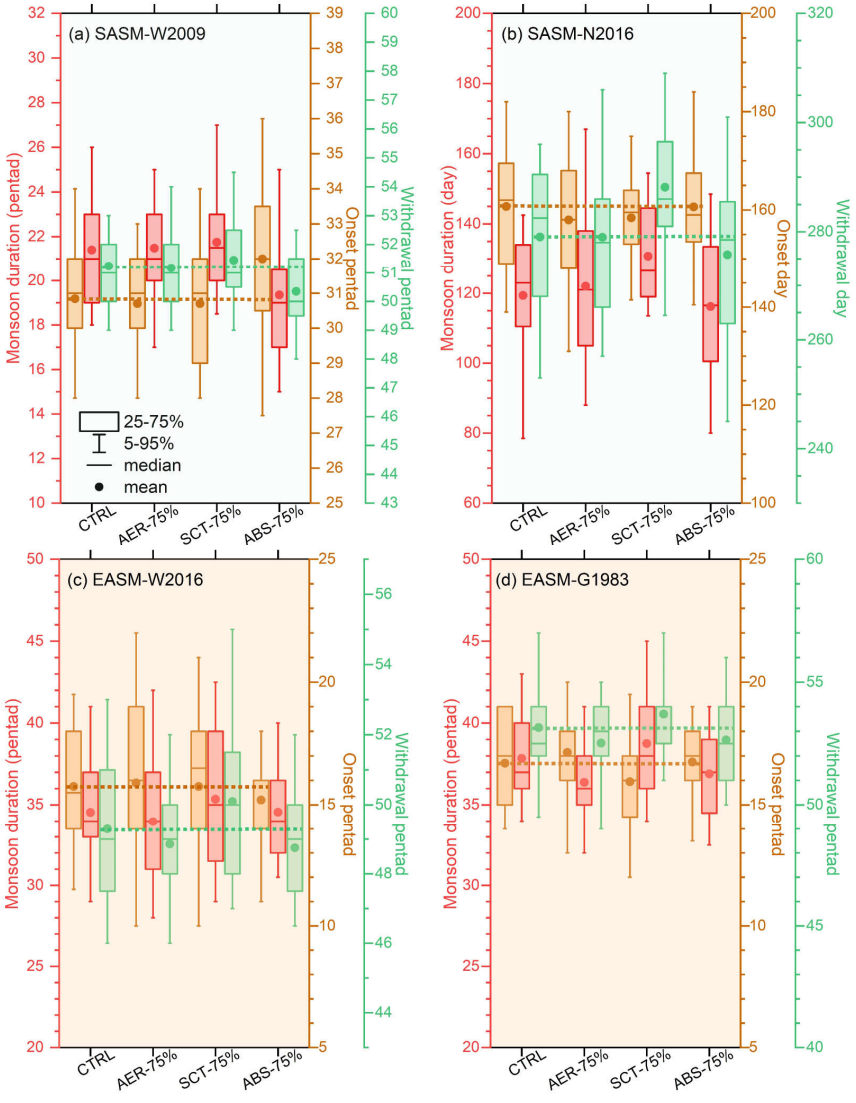

Figure 6: Same as Figure 4, but for the monsoon onset dates (yellow; unit: pentad for a, c and d, day for b), withdrawal dates (green; unit: pentad for a, c and d, day for b) and duration (red; unit: pentad for a, c and d, day for b).

https://doi.org/10.5194/egusphere-2023-407
Preprint. Discussion started: 28 March 2023

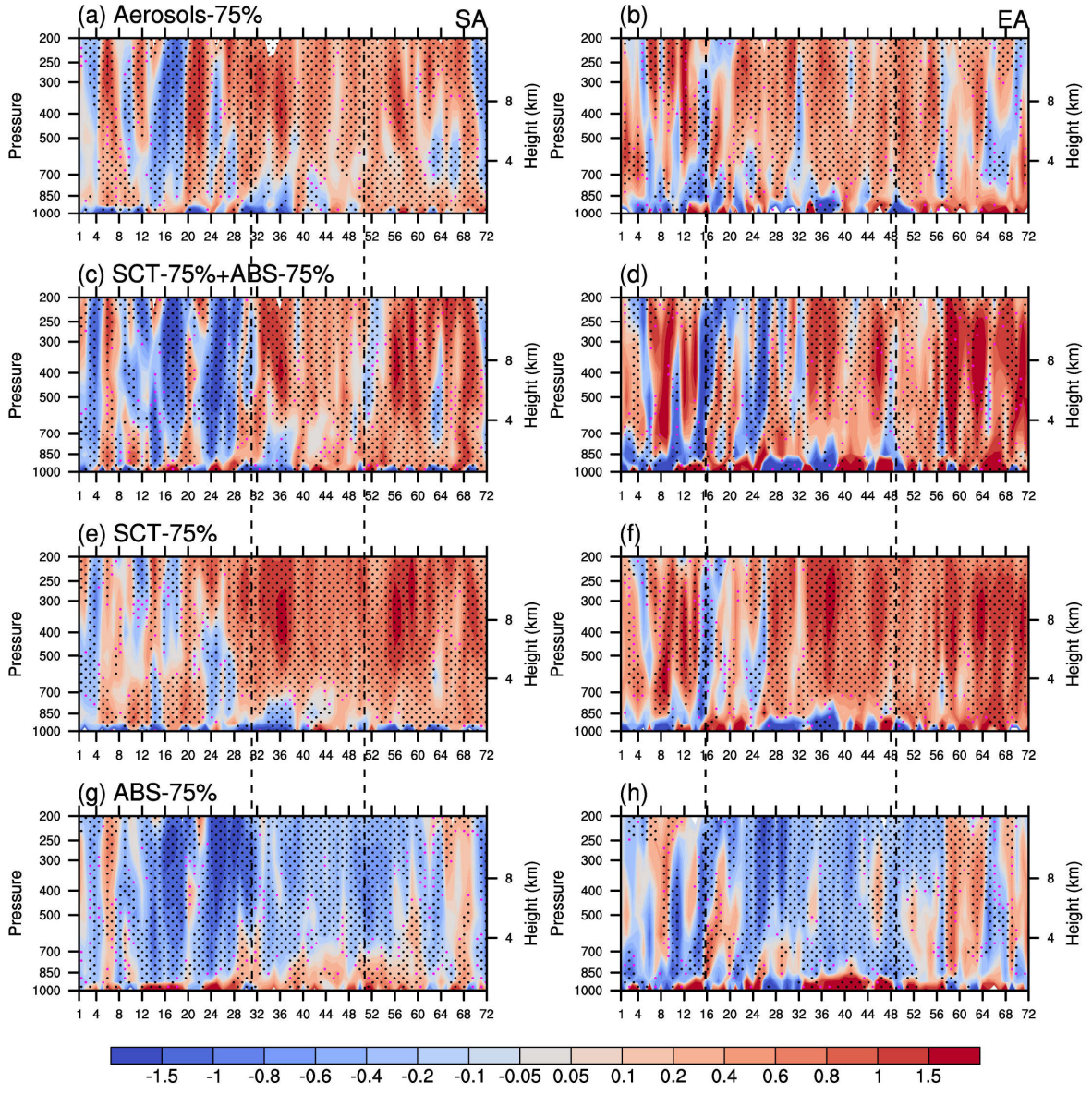

Figure 7: Time-altitude cross sections of the temperature (unit: K) responses to the reductions in total aerosols (a and b), SCT aerosols (e and f) and ABS aerosols (g and h) averaged over South Asia (a, c, e and g) and East Asia (b, d, f and h). The x-axis denotes the time (unit: pentad). The division of South and East Asia used here follows Iturbide et al. (2020) and is also shown in Fig. S1. Panels (c) and (d) are the sum of the impacts of the reductions in the SCT and ABS. The first and second vertical dashed lines in Panels (a), (c), (e) and (g) denote the monsoon onset and withdrawal pentad over South Asia in the control experiment based on the definition from W2009. The first and second vertical dashed lines in Panels (b), (d), (f) and (h) denote the monsoon onset and withdrawal pentad over East Asia in the control experiment based on the definition from W2016. Black and pink dotted regions denote where the temperature change is statistically significant at the 95% and 90% confidence level, respectively, according to a t-test.

https://doi.org/10.5194/egusphere-2023-407
Preprint. Discussion started: 28 March 2023

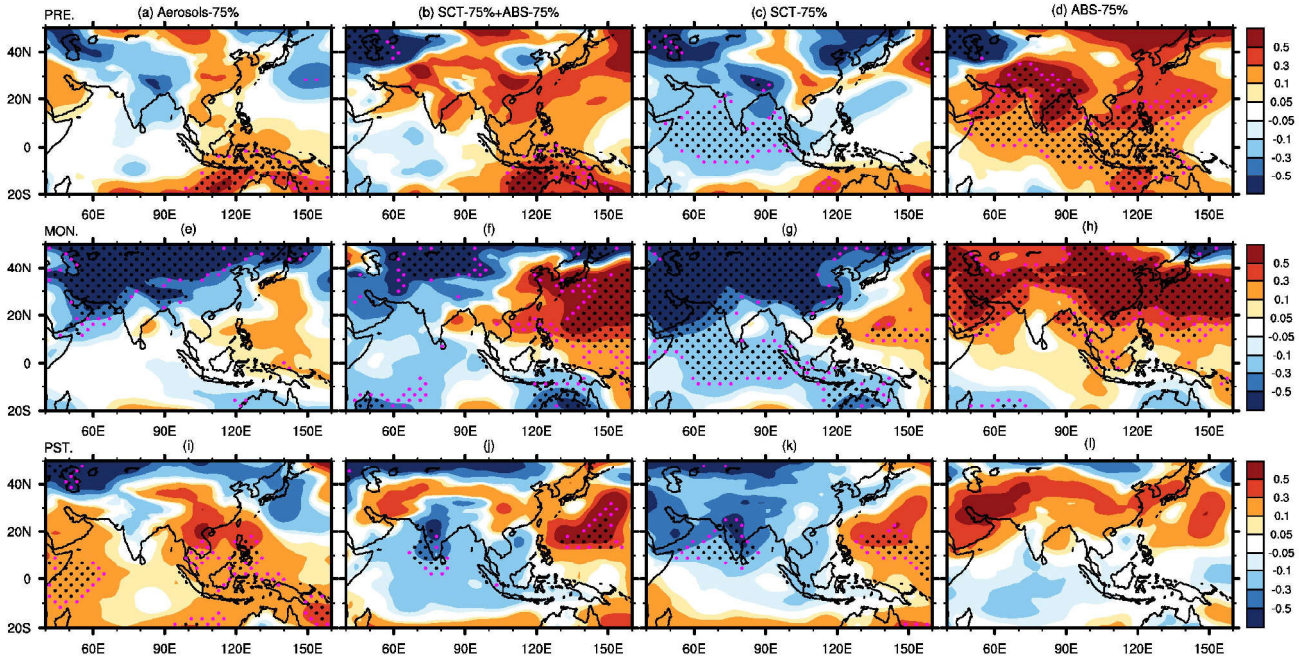

Figure 8: Spatial distributions of the sea level pressure (unit: hPa) responses to the reductions in total aerosols (a, e and i), SCT aerosols (c, g and k) and ABS aerosols (d, h and l) over Asia during pre-monsoon (April-May; a-d), monsoon (June-August; e-h) and post-monsoon (September-October; i-l) seasons. Panels (b), (f) and (j) are the sum of the impacts of the reductions in the SCT and ABS. Black and pink dotted regions denote where the sea level pressure change is statistically significant at the 95% and 90% confidence level, respectively, according to a t-test.

https://doi.org/10.5194/egusphere-2023-407
Preprint. Discussion started: 28 March 2023

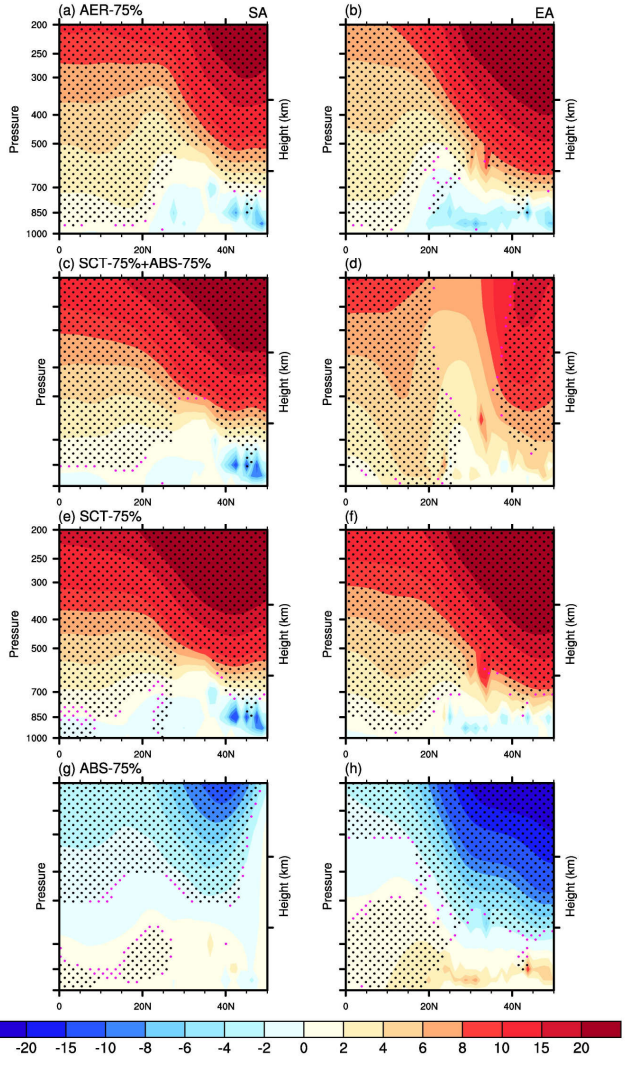

Figure 9: Zonal-mean geopotential height (unit: gpm) responses to the reductions in total aerosols (a and b), SCT aerosols (e and f), and ABS aerosols (g and h) during monsoon season over South Asia (70-90°E; a, c, e and g) and East Asia (100-120°E; b, d, f, h). Monsoon season is analyzed and based on the definitions from W2009 over South Asia and W2016 over East Asia. Panels (c) and (d) are the sum of the impacts of the reductions in the SCT and ABS. Black and pink dotted regions denote where the geopotential height change is statistically significant at the 95% and 90% confidence level, respectively, according to a t-test.

https://doi.org/10.5194/egusphere-2023-407
Preprint. Discussion started: 28 March 2023

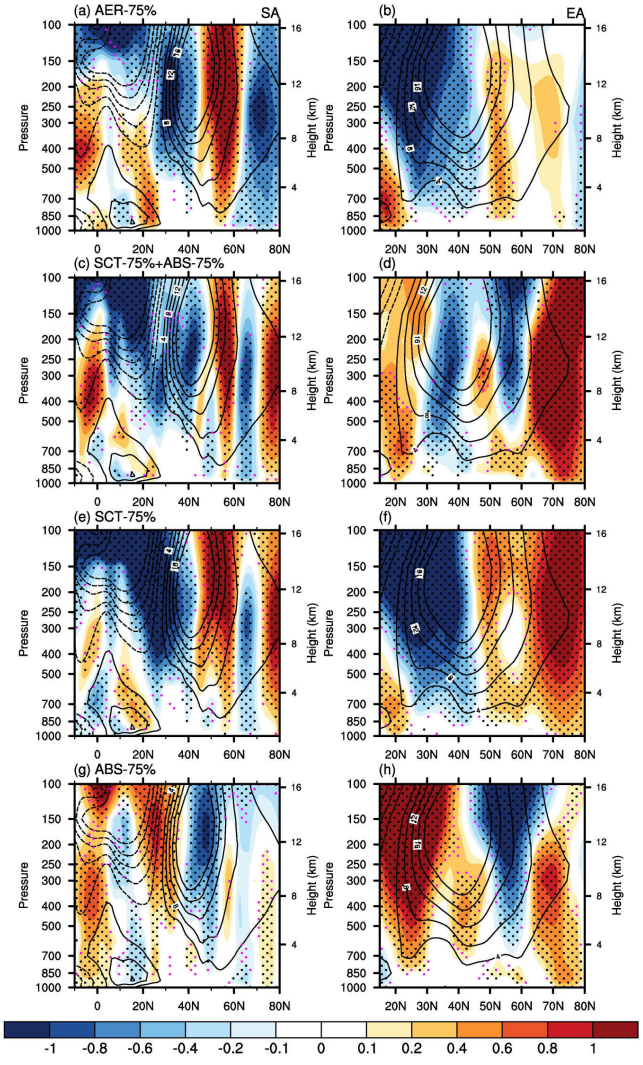

Figure 10: Same as Figure 9, but for the zonal-mean zonal wind (shading; unit: m s^{-1}; red and blue denote westerly and easterly wind, respectively) responses during monsoon season. Monsoon season is analyzed and based on the definitions from W2009 over South Asia and W2016 over East Asia. Black lines represent the climatological zonal wind from control simulations (unit: m s^{-1}; solid and dash lines denote westerly and easterly wind, respectively).

https://doi.org/10.5194/egusphere-2023-407
Preprint. Discussion started: 28 March 2023

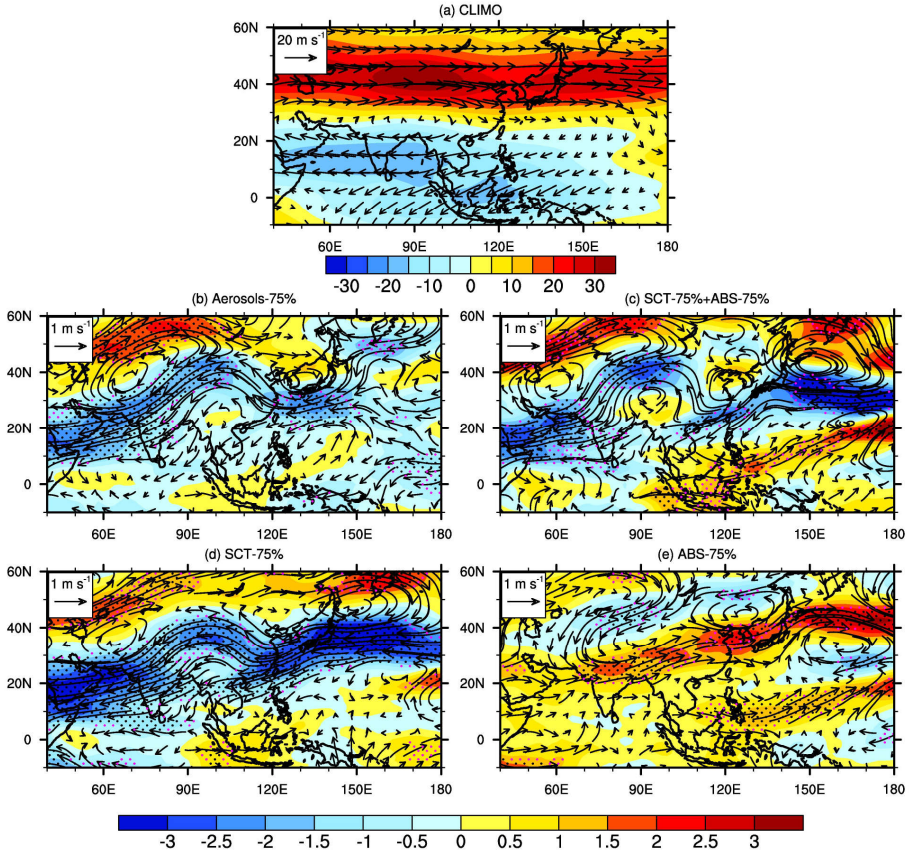

Figure 11: Spatial distributions of the 200-hPa zonal wind (shading; unit: m s^{-1}) and wind fields (vectors; unit: m s^{-1}) responses to the reductions in total aerosols (b), SCT aerosols (d) and ABS aerosols (e) over Asia during monsoon season (June-August). Panel (a) is the climatological 200-hPa zonal wind (unit: m s^{-1}) and wind fields (unit: m s^{-1}) from control simulations. Panel (c) is the linear addition of the impacts of the reductions in the SCT and ABS. Black and pink dot-ted regions denote where the zonal wind change is statistically significant at the 95% and 90% confidence level, respectively, according to a t test.

https://doi.org/10.5194/egusphere-2023-407
Preprint. Discussion started: 28 March 2023

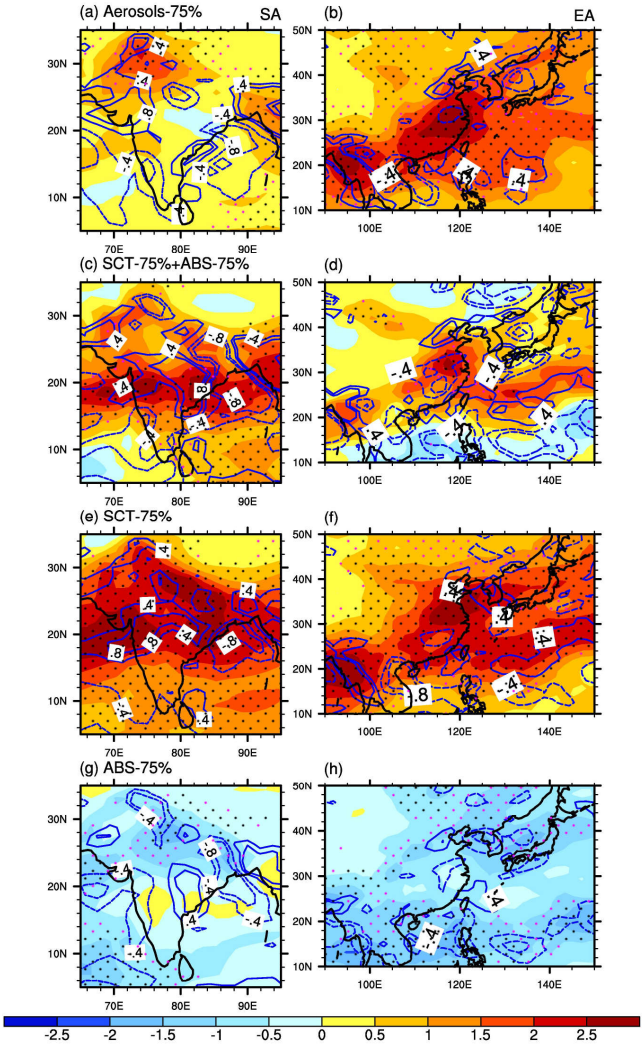

805 **Figure 12: Spatial distributions of the total column moisture flux (shading; unit: kg m^{-2} s^{-1}; red denote moisture convergence and blue denote divergence) and 850-hPa vertical velocity (contours; unit: -100×Pa s^{-1}) responses to the reductions in total aerosols (a and b), SCT aerosols (e and f) and ABS aerosols (g and h) during monsoon season over South Asia (a, c, e and g) and East Asia (b, d, f and h). Monsoon season is analyzed and based on the definitions from W2009 over South Asia and W2016 over East Asia. Panels (c) and (d) is the linear addition of the impacts of the reductions in the SCT and ABS. Black and pink dotted regions denote where**
810 **the total column moisture flux change is statistically significant at the 95% and 90% confidence level, respectively, according to a t-test.**

https://doi.org/10.5194/egusphere-2023-407
Preprint. Discussion started: 28 March 2023

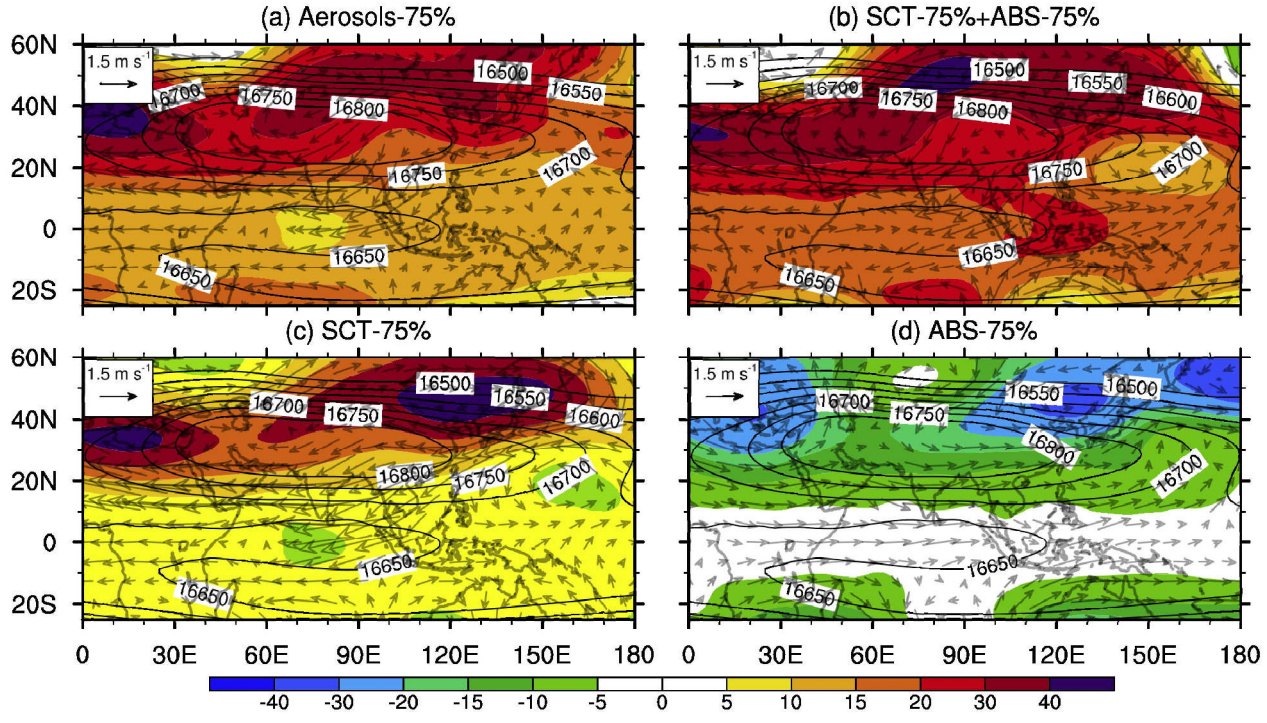

Figure 13: Spatial distributions of the 100-hPa geopotential height (shading; unit: gpm) and wind fields (vectors; unit: m s^{-1}) responses to the reductions in total aerosols (a), SCT aerosols (c) and ABS aerosols (d) over Asia during monsoon season (June-August). Panel (b) is the linear addition of the impacts of the reductions in the SCT and ABS. Black lines is the climatological geopotential height (unit: m) from control simulations, and the center value of South Asian High is more than 16800 gpm.